2014

QUARTZ CRYSTAL MICROBALANCE INVESTIGATION OF CELLULOSOME ACTIVITY FROM CLOSTRIDIUM THERMOCELLUM ON MODEL CELLULOSE FILMS

Shanshan Zhou
University of Kentucky, shs.zhou@hotmail.com

QUARTZ CRYSTAL MICROBALANCE INVESTIGATION OF CELLULOSOME
ACTIVITY FROM CLOSTRIDIUM THERMOCELLUM ON MODEL
CELLULOSE FILMS

THESIS

A thesis submitted in partial fulfillment of the requirements

for the degree of Master of Science in Chemical Engineering

in the College of Engineering at the University of Kentucky

By

Shanshan Zhou

Lexington, Kentucky

Director: Dr. Barbara L. Knutson, Professor of Chemical engineering

Lexington, Kentucky

2014

ABSTRACT OF THESIS

QUARTZ CRYSTAL MICROBALANCE INVESTIGATION OF CELLULOSOME
ACTIVITY FROM CLOSTRIDIUM THERMOCELLUM ON MODEL
CELLULOSE FILMS

The cost of deconstructing cellulose into soluble sugars is a key impediment to the commercial production of lignocellulosic biofuels. The use of the quartz crystal microbalance (QCM) to investigate reaction variables critical to enzymatic cellulose hydrolysis is investigated here, extending previous studies of fungal cellulase activity for the first time to whole cell cellulases. Specifically, the activity of the cellulases of *Clostridium thermocellum*, which are in the form of cellulosomes, was investigated. To clearly differentiate the activity of free cellulosome and cell-bound cellulosome, the distribution of free cellulosome and cell-bound cellulosome in crude cell broth at different growth stages of *C. thermocellum* (ATCC 27405) was quantified. Throughout growth, greater than 70% of the cellulosome in the crude cell broth was unattached to the cell. The frequency response of the QCM was shown to capture adsorption and hydrolysis of amorphous cellulose films by the whole-cell cellulases. Further, both crude cell broth and free cellulosomes were found to have similar inhibition pattern (within 0 - 10 g/L cellobiose). Thus, kinetic models developed for the cell-free cellulosomes, which allow for more accurate interfacial adsorption analysis by QCM than their cell-attached counterparts, may provide insight into hydrolysis events in both systems.

KEYWORDS: *C.thermocellum*, cellulosome, QCM, cellulose hydrolysis, inhibition

Shanshan Zhou
July 7, 2014

QUARTZ CRYSTAL MICROBALANCE INVESTIGATION OF CELLULOSOME
ACTIVITY FROM CLOSTRIDIUM THERMOCELLUM ON MODEL
CELLULOSE FILMS

By

Shanshan Zhou

Dr. Barbara Knutson
Director of Thesis

Dr. Thomas Dziubla
Director of Graduate Studies

July 7, 2014

ACKNOWLEDGMENTS

TABLE OF CONTENTS

LIST OF TABLES

LIST OF FIGURES

CHAPTER ONE

Introduction

Biofuel production from lignocellulose

Biofuels and biomass-derived commodity chemicals are renewable alternatives to fossil fuels. The development of low-cost and sustainable biorefinery technologies is the key factor in the further utilization of these biofuels. In this context, lignocellulose, the most abundant, sustainable and relatively low cost plant biomass in nature, is the most attractive feedstock for biofuel production. However, compared to biochemical production from soluble carbohydrates (i.e., sugar cane (sugar) and corn (starch)), the structure of lignocellulose makes the production of lignocellulosic biofuel more complicated.

In typical lignocellulosic biomass (Fig.1.1), cellulose, which is a long chain crystalline polymer that comprises glucose monomers, is the main structural constituent. Glucose molecules are linked by ß-1,4-glycosidic linkages and the polymer chains are joined together by hydrogen bonds, resulting in highly organized cellulose fibers (Kumar et al. 2009). This cellulose macrofibril is then wrapped by hemicellulose and lignin, forming cell walls to protect plants from outside attack. Most naturally occurring cellulose is crystalline, which is difficult to hydrolyze. Only about 1% of cellulose is in amorphous form, which is easier to decompose (Ruel et al. 2012). Unlike crystalline cellulose, which is an unbranched polymeric chain comprising a single type of monomer, hemicellulose is a highly branched amorphous polymer which contains various sugar monomers, with xylose, arabinose, mannose as the main components (Kumar et al. 2009, Rubin 2008, Jorgensen et al. 2007). Glucose and xylose are the most and second most abundant carbohydrate sugar in lignocellulosic biomass respectively, which are the essential for lignocellulosic fuel production (Zhang and Geng 2012). The amorphous structure and short branch chains makes hemicellulose easily decomposed by chemicals or enzymes. Meanwhile, lignin is most nondegradable component in lignocellulose. Lignin is across-linked polymer consisting of three alcohol monomers: p-coumaryl alcohol, coniferyl alcohol and sinapyl alcohol. The lignin content varies from plant species, which can range between 15% and 36% on the lignocellulosic biomass on a dry basis (Campbell and Sederoff 1996).
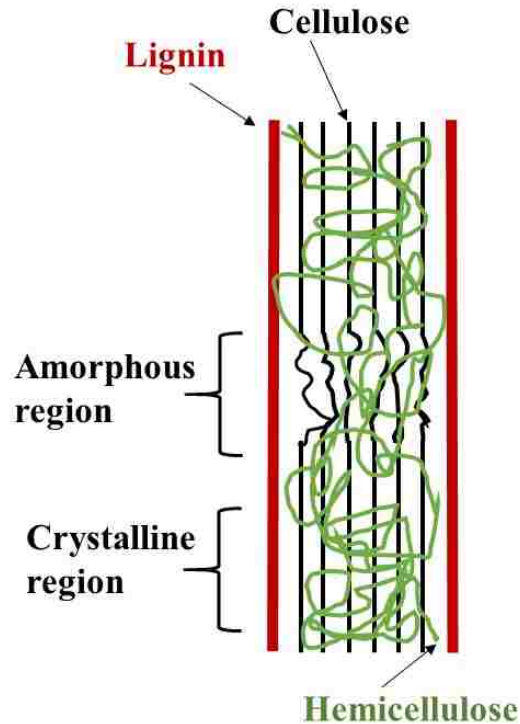
Figure 1.1 Structure of lignocellulose. The figure is adapted from Kumar et al. (2009).

A lignocellulosic biofuel production process using biochemical pathways (Fig.1.2) includes: pretreatment, hydrolysis, fermentation and purification. As mentioned before, hemicellulose and lignin are covalently linked and cover cellulose, which makes cellulose inaccessible to acid hydrolysis or enzymatic hydrolysis (using cellulases). Thus, pretreatment is the first and key step in lignocellulosic biofuel production. The main purpose of pretreatment is to remove the lignin and hemicellulose to make cellulose more accessible to enzymes or acid and improve hydrolysis efficiency. Pretreatment methods include physical (milling and grinding), physicochemical (steam pretreatment/autohydrolysis, hydrothermolysis, and wet oxidation), and chemical (alkali, dilute acid, oxidizing agents, and organic solvents) processes (Taherzadeh and Karimi 2007).

After pretreatment, the exposed cellulose is decomposed into glucose by enzymes or acid, which break up the ß-1, 4-glycosidic linkages. Glucose is then fermented into biofuels by microorganisms. Biofuels of high purity can be recovered from the fermentation broth in purification processes, such as distillation and adsorption (Kumar et al. 2009).
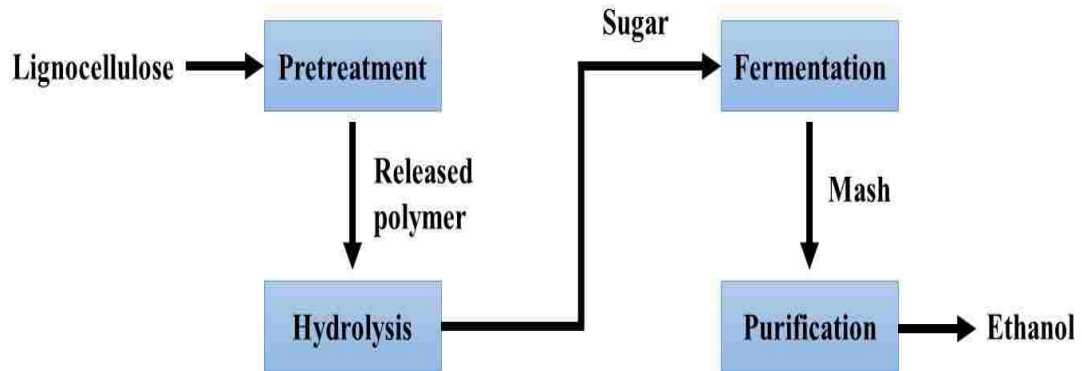
Figure 1.2 Schematic of lignocellulosic biofuel production. The figure is adapted from Taherzadeh and Karimi (2007).

Despite the potential of lignocellulosic biofuels, the high cost of pretreatment and low efficiency of enzymatic hydrolysis still remain as the key impediment for industrializing this process (Rubin 2008, Ding et al. 2012). Efficient pretreatment removes lignin and hemicellulose, improving cellulose accessibility (Taherzadeh and Karimi 2007). Furthermore, the crystallinity of cellulose is reduced after pretreatment, which makes cellulose more amenable to hydrolysis (Himmel, Ding et al. 2007). Also, the surface area and porosity of cellulose are improved by effective pretreatment, providing more active site for cellulases (Yang, Dai et al. 2011). The selected pretreatment method should depend on the plant types (different lignin content) and hydrolysis process(Chang et al. 2001). Improving pretreatment efficiency to enhance the conversion of cellulose is an active area of research.

A promising technology for low cost and high yield biofuel production is "consolidated bioprocessing" (CBP), which combines the enzyme production, lignocellulose hydrolysis and microbial sugar fermentation in a single process (Lynd et al. 2005). However, no single existing microorganism has been found to efficiently hydrolyze cellulose to soluble sugars and simultaneously ferment these soluble sugars (Xu, Singh et al. 2009). A promising microorganism is *Clostridium thermocellum,* which is both cellulolytic and ethanologenic (Xu et al. 2010). However, the application of *C.thermocellum* is limited since the optimal reaction conditions (with respect to temperature and pH, for example) differs for cellulose hydrolysis and fermentation processes (Jorgensen et al. 2007). Also, the fermentation product (ethanol) can be toxic to the microorganisms (Herrero and Gomez 1980). Thus, further development of CBP should involve deeper understanding of the mechanism of microbial strain metabolism and developing more efficient microorganisms with capability for cellulose hydrolysis

and ethanol production. Despite the challenges of CBP, development of CBP would have the benefits of reducing capital investment, maintenance and operation costs in the biorefinery. Furthermore, the hydrolysis product can be consumed by fermentation in time, resulting in low hydrolysis product concentration, less hydrolysis product inhibition on cellulase and thus higher hydrolysis efficiency (Hasunuma and Kondo 2012, Xu et al. 2009).

Cellulase system

Developing efficient hydrolysis techniques is still a major challenge facing economical lignocellulosic biofuel production. Typically, the conversion of cellulose into fermentable sugar can be carried out by acid or cellulases. Advances in enzymatic hydrolysis technologies are required to achieve a low cost and high efficiency biorefinery. In contrast to acid hydrolysis, enzymatic hydrolysis has high selectivity and high glucose yield, due to the specificity of the cellulase enzymes used to decompose cellulose into glucose. Furthermore, enzymatic hydrolysis is usually conducted at low temperature (45-50°C) and a mild pH (4.2-5.8) (Pardo and Forchiassin 1999), which requires less energy relative to acid hydrolysis and avoids corrosion issues (Sun and Cheng 2002). Also, the inhibition of fermentation by hydrolysis byproducts is not as severe as acid hydrolysis.

Microorganisms that are capable of producing enzymes to degrade insoluble cellulose can be divided into bacteria and aerobic fungi. Usually, a fungal cellulase consists of a catalytic domain, which catalyzes cellulose degradation by acid-base catalysis, and a cellulose binding domain (CBD), which can bind to the specific sites on cellulose surface through hydrogen bonding and van der Waals interactions (Xi et al. 2013) and make the cellulose accessible to the catalytic domain. These two domains are connected by a poly-linker (Fig.1.3).

Although the cellulose binding domain (CBD) is non-catalytic, the role of the CBD in hydrolysis activity improvement cannot be neglected. In the absence of the CBD, the ability of cellulase to hydrolyze insoluble substrates dramatically decreases (Boraston et al. 2004). The CBD generally has three functions: i) a targeting function (Carrard 2000): CBD can target to the specific region on cellulose substrate through hydrogen bond and van der Waals interactions ; ii) a proximity effect (Bolam et al. 1998): The targeting of CBD to the substrate brings the catalytic domain close to the substrate

surface, which concentrates the cellulase on the substrate surface and then increases hydrolysis rate; iii) a disruptive function (Gao 2001): Some CBDs even show the ability of break down cellulose, which makes it easier for the action of catalytic domain. However, this phenomenon is not very common (Boraston et al. 2004).
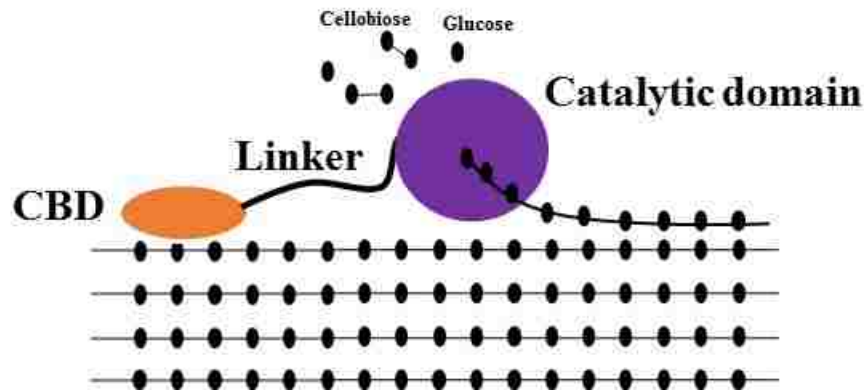
Figure 1.3 Fungal cellulase structure. The figure is adapted from Xi et al. (2013).

Based on the modes of action and structural properties of the catalytic domain, cellulases, which cleave ß-1, 4-glycosidic linkages, can be classified into exo-glucanases and endo-glucanases. Typically, an endo-acting enzyme has cleft-shaped open active sites (Maki et al. 2009), which allow endo-glucanases to break down the glycosidic linkage at internal amorphous regions of the cellulose chain. Meanwhile, exo-glucanases (cellobiohydrolases), like other exo-acting enzymes, have tunnel-shaped close active sites preventing the enzyme from adhering to the substrate (Maki et al. 2009). Therefore, exo-glucanases can only cleave the glycosidic linkages from either reducing end or non-reducing ends of the cellulose chain, producing glucose or cellobiose. Exo-glucanases can processively hydrolyze a single chain, which offers great hydrolysis efficiency (Zhong et al. 2007).

Overall, the bioconversion of cellulose into fermentable sugar results from the synergistic action of three types of enzymes: exo-glucanase, endo-glucanase and ß-glucosidase (Xi et al. 2013, Lynd et al. 2002, Li 2012) (Fig.1.4 A): Exo-glucanase (cellobiohydrolase) processively decompose crystalline cellulose from chain end and release cellobiose as main component, which expose and provide underlying amorphous regions on which endo-glucanases can act; Endo-glucanases break down the network of cellulose, and generate various oligosaccharides, which create new chain ends on which exo-glucanases can act; ß-glucosidase decomposes cellobiose into glucose, which relieves the inhibition of cellobiose on exo-glucanases activity.
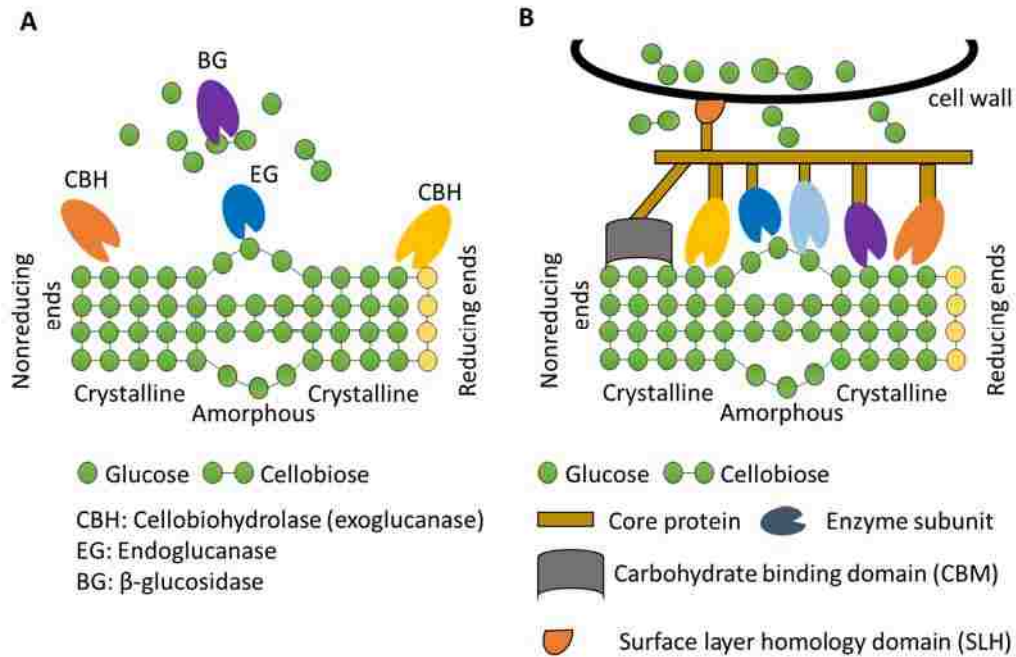
Figure 1.4 Schematic of cellulose hydrolysis by non-complexed (A) and complexed (B) cellulase systems. The figure is adapted from Ratanakhanokchai et al. (2013).

Typically, cellulase systems are categorized by two types: complexed cellulases or non-complexed cellulases (Lynd et al. 2002). Non-complexed cellulases are produced by fungi and some aerobic bacteria such as *Phanerochaete chrysosporium and Trichoderma reesei*. Non-complexed cellulases are secreted freely and separately from the cells. Meanwhile complexed cellulases are multi-protein complexes, in which enzymes combine and anchor on the surface of the bacteria by non-catalytic proteins. This kind of multi-protein complex is also termed as a cellulosome. Complexed cellulases are often produced by anaerobic bacteria, such as *Clostridium thermocellum*. Due to the structural differences between complexed and non-complexed cellulases system, they interact differently with cellulose (Fig.1.4), which result in different hydrolysis abilities.

Clostridium thermocellum: a potential cellulosome source for lignocellulose hydrolysis

Clostridium thermocellum, an anaerobic, thermophilic, Gram-positive bacterium, is recognized for its potential as cellulolytic organism, producing highly efficient complexed cellulase (cellulosome) for cellulose degradation (Zhang and Lynd 2005). *C. thermocellum* can hydrolyze cellulose into cellobiose and cellodextrins, which is then transferred into the cell and metabolized into ethanol, acetic acid, lactic acid, ,

6

formic acid, hydrogen and carbon dioxide (Demain et al. 2005). This makes *C.thermocellum* a potential microorganism for "consolidated bioprocessing (CBP)", which combines the enzyme production, enzymatic hydrolysis and sugar fermentation in one single step (Xu, Qin et al. 2010).

The fundamental structure of the cellulosome, which has a complex protein composition, has been revealed as important proteins are identified through gene cloning and sequencing (Raman et al. 2009). As shown in Fig.1.5, the cellulosome also has various catalytic domains, which have the same hydrolysis ability as fungal cellulase. The difference between fungal cellulase (non-complexed cellulase) and cellulosome (complexed cellulase) is that cellulosomal catalytic domains are linked with dockerin domains instead of cellulose binding domain to form an enzymatic unit (Tokatlidis et al. 1991, Morag et al. 1992). The function of dockerin domains is to assemble these catalytic domains into a complex through interaction with the cohesin domains on scaffoldin (Gerngross et al. 1993, Tokatlidis et al. 1991). Typically, the scaffoldin of *C.thermocellum* consist of nine copies of type-I cohesin domain, a Family-IIIa cellulose binding domain (CBD) and a type-II dockerin domain (Demain, Newcomb et al. 2005). Similar to the CBD of fungal cellulase, the Family-IIIa CBD is responsible for the targeting of the substrate and has the ability to interfere with the noncovalent interactions between cellulose chains (Din et al. 1994, Din et al. 1991). The type-I cohesin domains interact with the type-I dockerin domains, which is linked with catalytic domains, through calcium dependent binding (Choi and Ljungdahl 1996, Yaron et al. 1995). Meanwhile, the catalytic domains together with scaffoldin are attached to the cell surface mediated by the type-II dockerin domains, which bind to the type-II cohesin domains of the cell-surface anchoring proteins, SdbA, Orf2p and OlpB (Fujino et al. 1993). These S-layer proteins all contain one SLH (S-layer homologous) domain and one, two, four type-II dockerin domains, respectively, which recognize the dockerin domains of the scaffoldin (Demain et al. 2005, Bayer et al. 1998). The forth anchoring protein, OlpA, only contains one SLH domain and type-I cohesin domain, which recognizes the dockerin domains of the enzymatic unit. Thus, the enzymatic unit can directly attach to the cell surface through OlpA protein.
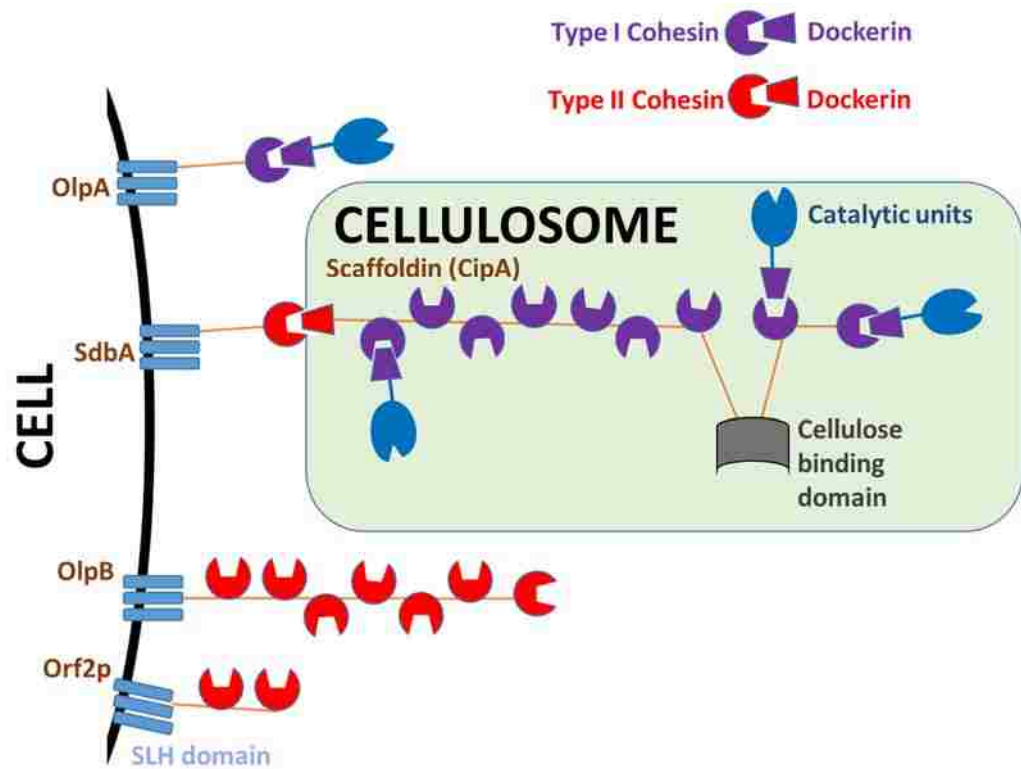
Figure 1.5 Schematic of the cellulosome structure. The figure is adapted from Raman et al. (2009).

The special architecture of cellulosome from *C. thermocellum* is believed to contribute to its higher hydrolysis activity than fungal cellulase. By assembling the catalytic domains in a complex, the cellulosome can ensure that the ratio between synergistic enzymes remains optimum on the substrate surface, which guarantees a constant highly efficient degradation rate (Lynd et al. 2002, Tuka et al. 1992). Concomitantly, catalytic domains on the same scaffoldin and scaffoldins attached to different sites on the cell surface are well spaced, which eliminates the competition between catalytic domains on the same site acting on the substrate. Furthermore, of the 22 catalytic domains on the cellulosome, at least nine are endo-glucanases, four are exo-glucanases, and five are hemicellulases, one of which is chitinase, and one of which is lichenase (Lynd et al. 2002, Demain et al. 2005). The presence of other enzymes, particularly the hemicellulases, which can help to remove the hemicellulose and break down lignocellulose fiber, makes cellulose more accessible to cellulase and leads to fast degradation of the plant cell materials (Himmel et al. 2007, Taherzadeh and Karimi 2007) .

The cellulosome may exist in both cell-associated and extracellular forms.

8

Previous studies suggest that the cellulosome of *C. thermocellum* are cell-associated (attached to the cell surface) in the early exponential growth phase (Bayer et al. 1985). The cell-associated cellulosome is then detached from cell surface as the life cycle proceeds. Most cellulosomes are in extracellular form in the stationary phase (Demain et al. 2005). Furthermore, a recent work (Lu et al. 2006) has shown that the crude cell broth of *C .thermocellum* (cell-bound cellulosome and cell-free cellulosome both exist) exhibited 2.3-4.5 fold higher hydrolysis ability than cell-free cellulosome. Considering the separation cost and activity lost involved in enzyme purification, crude cell broth of *C.thermocellum* should be more economic cellulase source for industry production.

Lignocellulose hydrolysis model

The main challenges to efficient lignocellulosic fuel production include high pretreatment cost and low hydrolysis efficiency. Understanding the interaction of the cellulosome with lignocellulosic substrate during the hydrolysis is useful for designing or optimizing the hydrolytic process in industry. Multiple mathematical models have been developed to describe measurements of bulk cellulose hydrolysis in response to variables such as enzyme loading, temperature, and pretreatment (Bansal et al. 2009, Chang and Holtzapple 2000, Vasquez et al. 2007, Kim and Holtzapple 2006). These models can be divided into: empirical models (Zhou et al. 2009, Turon et al. 2008, Ohmine et al. 1983), Michaelis-Menten based models (Gusakov et al. 1985b, Shin et al. 2006, Drissen et al. 2007), fractal kinetic model (Xu and Ding 2007, Valjamae et al. 2003, Kopelman 1988), and jamming kinetic model (Xu and Ding 2007, Bansal et al. 2009).

Empirical models are used most commonly in predicting hydrolysis under various reaction condition and substrate properties, without knowing the mechanistic changes of the hydrolysis process. Usually, empirical models are developed by fitting a mathematical equation to large data collection that describes the extent of hydrolysis or hydrolysis rate with respect to time or independent reaction parameters. To date, many empirical models have been developed, which have shown that hydrolysis efficiency depends on pH, temperature and substrate properties (lignin content, degree of polymerization, crystallinity, accessible surface area)(Ahola et al. 2008b). Furthermore, the empirical models can be used for initial hydrolysis rate estimation, reaction conditions optimization and pretreatment method optimization by characterizing the

substrate properties using DRIFT (Diffuse reflectance infrared fourier transform) spectra (Bansal et al. 2009). It should be noted that empirical models can only apply to the experimental condition under which they are developed.

The Michaelis-Menten model (Michaelis and Menten 1913) describes the kinetics between a single substrate and single enzyme, which is the simplest enzyme-catalyzed reaction. As shown in Fig.1.6 (A), it postulates that the enzymatic reaction proceeds through the reversible formation of an enzyme-substrate (ES) complex. An irreversible enzymatic reaction releases product (P) and free enzyme (E). Most analyses of this reaction sequence assume that that rate of ES complex formation is much faster than the reaction step, thus the product formation step determines the overall reaction rate.
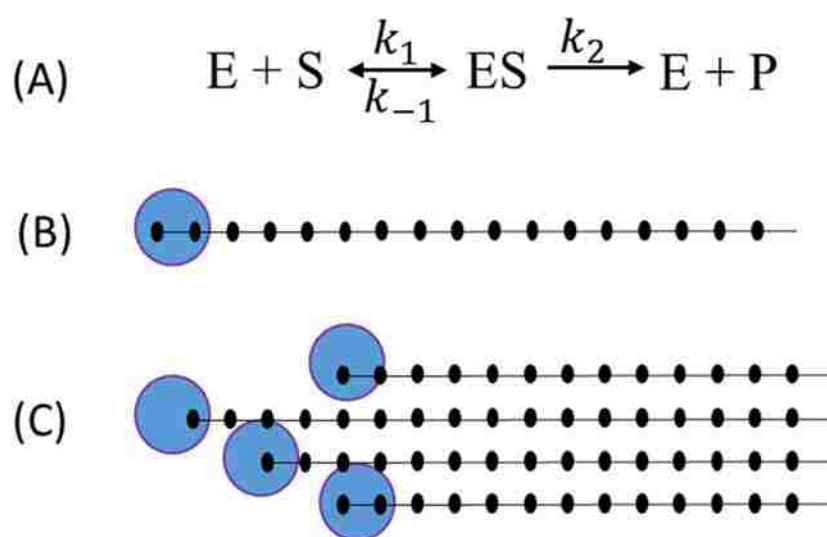
Figure 1.6 Schematic for Michaelis-Menten (A), fractal (B) and jamming kinetics (C). The figure is adapted from Xu and Ding (2007).

Based on Michaelis-Menten model, four types of enzyme inhibition are proposed (Fig.1.7): (i) Competitive inhibition: Inhibitor (I) competes with substrate for enzyme active site by forming enzyme-inhibitor complex (EI)(Shuler and Kargi 2002); (ii) Uncompetitive inhibition: Inhibitor only binds to the enzyme-substrate complex to reduce [ES]; (iii) Noncompetitive inhibition: Inhibitor can bind to the allosteric sites of either enzyme or enzyme-substrate complex, which prevents the product formation; (iv) Mixed typed: this type of inhibitor is similar to noncompetitive inhibitor, except that noncompetitive inhibitor has an equal affinity for the enzyme and the enzyme-substrate complex and mixed inhibitor has greater affinity for one of them. However, these Michaelis-Menten based models are derived for homogenous reaction systems, where and the substrate is soluble and all of the substrate is available to the enzyme. Therefore, additional assumptions accounting for the heterogeneity are needed, when Michaelis-

Menten based models is applied to enzymatic hydrolysis of insoluble substrate, which is a heterogeneous reaction.

(i) Competitive

$$E + S \xrightleftharpoons[k_{-1}]{k_1} ES \xrightarrow{k_2} E + P$$

$$+$$

$$I$$

$$k_i \uparrow\downarrow k_{-i}$$

$$EI$$

(ii) Uncompetitive

$$E + S \xrightleftharpoons[k_{-1}]{k_1} ES \xrightarrow{k_2} E + P$$

$$+$$

$$I$$

$$k_i \uparrow\downarrow k_{-i}$$

$$ESI$$

(iii) Noncompetitive

$$E + S \xrightleftharpoons[k_{-1}]{k_1} ES \xrightarrow{k_2} E + P$$

$$+ \qquad +$$

$$I \qquad I$$

$$k_i \uparrow\downarrow k_{-i} \qquad \downarrow K_I$$

$$EI + S \xrightleftharpoons[k_{-1}]{k_1} ESI$$

(iv) Mixed-type

$$E + S \xrightleftharpoons[k_{-1}]{k_1} ES \xrightarrow{k_2} E + P$$

$$+ \qquad +$$

$$I \qquad I$$

$$k_i \uparrow\downarrow k_{-i} \qquad k'_i \uparrow\downarrow k'_{-i}$$

$$EI + S \xrightleftharpoons[k_{-1}]{k_1} ESI$$
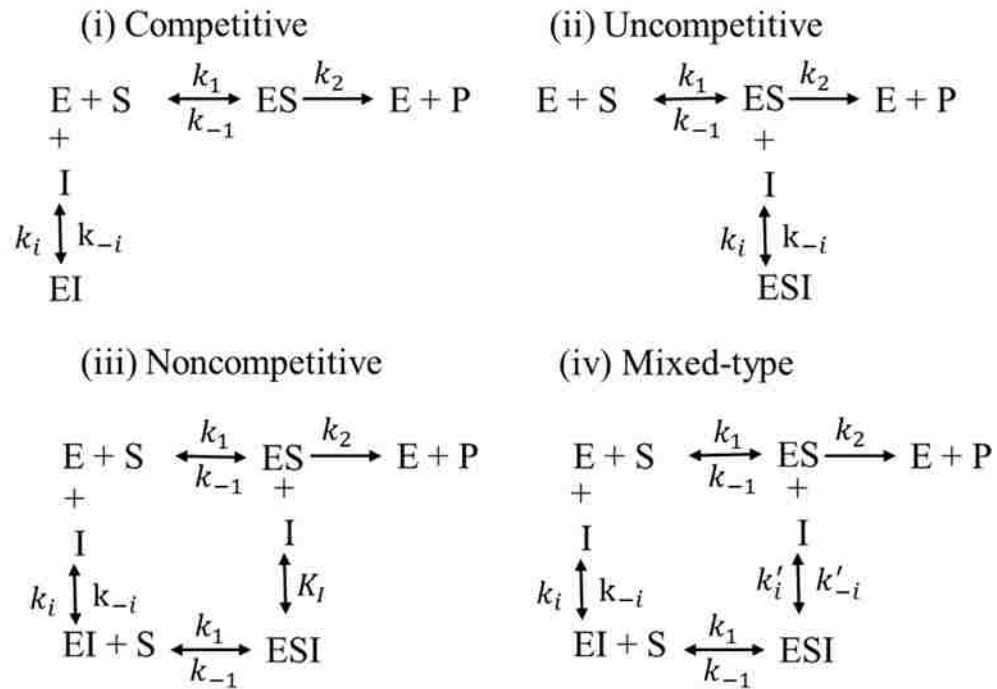
Figure 1.7 Four types of enzyme inhibition mechanism

Fractal kinetics is an effective approach to modeling reactions that are diffusion limited, dimensionally restricted, or occur on fractal surface (Valjamae et al. 2003). As shown in Fig.1.6 (B), the cellulase (ellipsoid) acts on the cellulose chain end, and moves along the chain in one direction as it cleaves the ß-1,4-glycosidic linkages (Xu and Ding 2007). This one-dimensional heterogeneous reaction can be described by fractal kinetics. The key point for developing fractal kinetics is that the rate constant is time-dependent (Kopelman 1988), which can be expressed as:

$$g = kt^{-f} \quad 0 < f < 1 \tag{1.1}$$

where k is homogenous reaction rate constant and f represents fractal dimension. By applying this rate constant expression to the classic Michaelis-Menten model (Fig. 1.6(A)), the expression for Michaelis-Menten model with fractal kinetic is developed as (Xu and Ding 2007):

$$\frac{k_2[E]t^{1-f}}{1-f} = [P] - K_m \ln\left(1 - \frac{[P]}{[S]}\right) \tag{1.2}$$

Jamming kinetics further consider the effect of enzyme size on the kinetics of the heterogeneous reaction. Because the cellulase molecule is larger than the distance between cellulose chains, cellulase could block the attachment site on the cellulose surface from other cellulases (Fig 1.6 (C)) (Xu and Ding 2007). Like a traffic jam, the

cellulase ahead will stop the cellulase behind it and affect the hydrolysis rate. As the cellulase concentration increases, these effect will become more significant. The jamming kinetics can be expressed as:

$$(1 - \frac{[E]}{j[S]})\frac{k_2[E]t^{1-f}}{1-f} = [P] - K_m\ln(1 - \frac{[P]}{[S]}) \qquad (1.3)$$

where j is the jamming parameter which is found to be around 0.0004 (Bansal et al. 2009).

Quartz crystal microbalance with dissipation (QCM-D)

In order to improve the design enzymatic hydrolysis processes, versatile tools to investigate the enzyme-substrate interactions and catalytic properties of cellulases under a broad range of hydrolysis conditions are needed. The quartz crystal microbalance (QCM-D) is a powerful interfacial technique for measuring enzymatic hydrolysis, which allows for monitoring in situ and in real time the binding and catalytic activity of cellulases on model cellulose substrates. QCM-D can measure the cellulose substrate mass change with time during hydrolysis based on mass sensing, which contributes to a kinetic profile of the reaction. Furthermore, it can capture the adsorption and desorption processes on the surface, which can be used to quantify how cellulases interact with the cellulose surface during hydrolysis.

The fundamental principle of QCM is the inverse piezoelectric effect, which is a natural property of crystal materials. By applying a certain voltage on the quartz sensor, which is covered with metal electrodes on the upper and lower sides, mechanical deformation is generated. Different voltages lead to different extents of mechanical deformation. Therefore, the application of alternating electric field on the quartz sensor results in a cyclical deformation, which is generated at the same frequency as the applied voltage. If this deformation frequency matches the crystal's inherent resonant frequency (f), an acoustic wave is generated (Reviakine et al. 2011). Thus, the surface event on the QCM sensor can be probed by its acoustic wave propagation properties variation, which can be converted into electrical signal through transducers (Ferreira et al. 2009).

Typically, a QCM sensor is an AT-cut thin (~0.1mm) quartz disk, which is cut at an angle of $35.15°$ to the optical Z-axis (Wegener et al. 2001). Depending on the relative position between cut angle and crystal lattice, the crystal shows different kinds of oscillation when an alternating voltage is applied (Reviakine et al. 2011). An AT-cut

QCM sensor with circular geometry oscillates in the thickness shear mode (TSM), where the upper and lower surface of the quartz sensor move in lateral and antiparallel directions (Fig.1.8)(Ferreira et al. 2009). Therefore, multiple acoustic waves that propagate in the direction vertical to the sensor surface is produced and their wavelengths (λ) are equal to 2d/n, where d is the thickness of QCM sensor and n is the overtone order. Since surface electrodes can excite only odd harmonics, therefore n = 1, 3, 5, ...(Wegener et al. 2001). Since the acoustic wave velocity (v) is defined as product of frequency (f) and wavelength ($\lambda = 2d/n$), the resonance frequency can be expressed as:

$$f_n = nv/2d \tag{1.4}$$

when n=1, the fundamental resonance frequency (f_o) is obtained. From the equation above, the dependence of f_o on the sensor thickness is clear. For example, the f_o of a common QCM sensor is 5 MHz, and its thickness is about 330 μm (Dixon 2008).
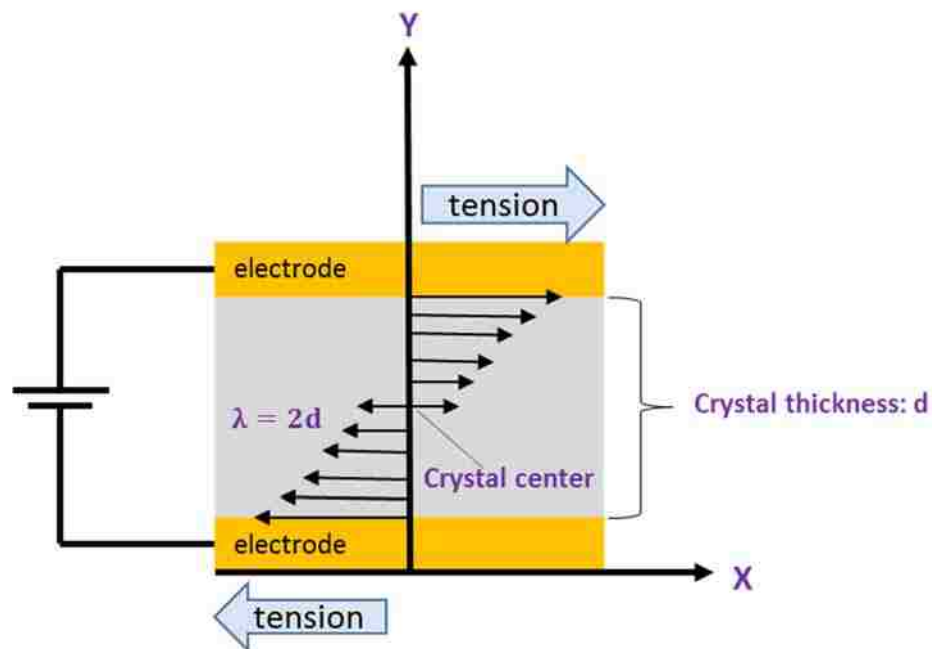
Figure 1.8 AT-cut QCM sensor oscillation mode. The figure is adapted from Ferreira et al. (2009).

The principle of the microbalance is that the sensor mass change, Δm, and resonance frequency change, Δf, are linearly related, as derived by Sauerbrey (Sauerbrey 1959). Any mass bound to the sensor surface increases the sensor's thickness, which decreases the resonance frequency according to Eq. 1.4 Thus, by relating the mass of the sensor ($m = A * d * \rho$, where A is the sensor area, ρ is the quartz density) with Eq. 1.4, the Sauerbrey equation is developed:

$$\Delta m = -\frac{C}{n}\Delta f \tag{1.5}$$

where n is the overtone order, $C = \frac{d\rho}{f_0}$ is the mass sensitivity constant. The negative sign in Eq. 1.5 indicates that an increase of mass will result in the decrease in frequency. For crystals with f_o=5 MHz, C is 18 Hz^{-1} ng cm^{-2} (Dixon 2008), which shows that this quartz microbalance has really high level of sensitivity (the unit of mass is ng). The Sauerbrey equation only applies when the following conditions are satisfied: (i) the added mass is uniformly deposited on the crystal surface. (ii) the added mass is rigidly adsorbed to the surface with no slip or deformation imposed by the oscillating surface. (iii) the bound mass is much smaller the crystal mass i. e., $\Delta f/f \ll 1$(Rodahl et al. 1995).

In liquid environments, the Sauerbrey equation is no longer satisfied since the assumption that the added mass is rigidly adsorbed to the surface is violated, due to the viscoelastic dissipation (Dixon 2008). Thus, the interpretation of mass change should include the film viscoelasticity (Hu 2009), which can be characterized by dissipation factor (D) and expressed as:

$$D = \frac{E_{Dissipated}}{2\pi E_{Stored}} \tag{1.6}$$

where $E_{Dissipated}$ is the energy dissipated during one oscillatory cycle and E_{Stored} is the energy stored in the oscillating system. Typically, under the vacuum or gaseous environment, the dissipation factor is about 10^{-6} to 10^{-4} (Rodahl et al. 1995). Therefore, the viscoelastic contribution can be neglect if the dissipation factor is small enough ($\sim 10^{-6}$), even in liquid environment.

Enzymatic kinetic of cellulose hydrolysis monitoring by QCM-D

Turon et al. (2008) were the first to report the study of enzymatic cellulose hydrolysis using QCM-D. As frequency change reflects the mass change of cellulose surface and dissipation change indicates the morphology and viscoelasticity change of the surface, their experiment results (Fig. 1.9) revealed four distinct stages during hydrolysis process:

(i)   Binding stage: a quick drop in frequency and a rapid increase in dissipation due to adsorption of enzyme onto the cellulose surface.

(ii)   Transition stage: enzyme hydrolysis begins to compete with adsorption which result in a minimum in frequency

(iii)   Enzyme hydrolysis: the frequency increases and passes through maximum rate

as cellulose is degraded by enzyme, while dissipation keeps increasing and goes through a maximum point before decreasing.

(iv)   Substrate depletion: frequency and dissipation reaches plateau as accessible cellulose is completely consumed.
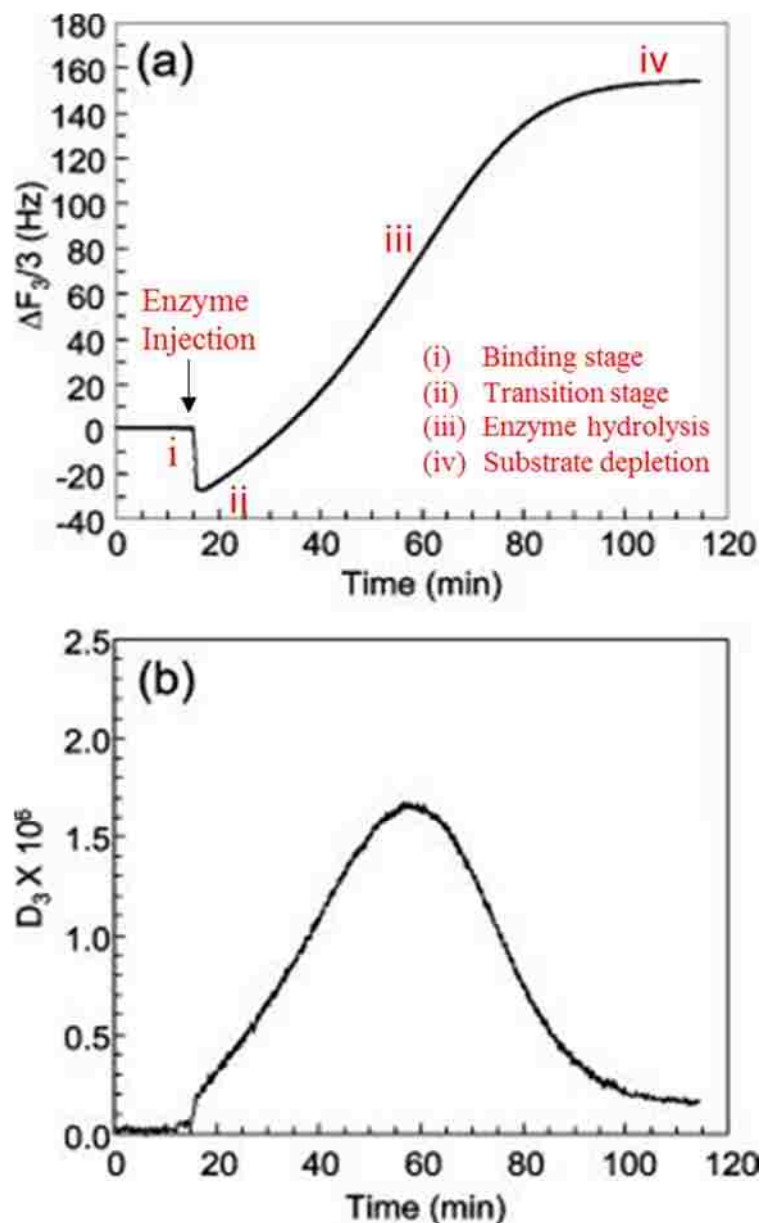
Figure 1.9 Frequency (a) and dissipation (b) profile during enzymatic hydrolysis on cellulose thin film. The figure is modified from Turon et al. (2008).

The work of Rojas group demonstrated that quartz crystal microbalance with dissipation (QCM-D) is a viable method to determine cellulase activity, which allows for monitoring in situ and in real time the cellulase binding and activity on model cellulose substrates. This tool can also be applied to study the effects of variables critical to cellulose hydrolysis, such as the cellulase system, the properties of cellulose substrate,

15

temperature, and pH.

The properties of the model cellulose thin film plays an important role in investigating cellulose activity by QCM. The degree of crystalinity, chemical composition, morphology, pore size distribution and specific surface area (Rojas et al. 2007) affect the efficiency of cellulase hydrolysis. To deposite celluose on a surface, series of cellulose-soluble solvents have been used to produce celluose solution, which result in regenerated celluose films with various crystillinities depending on the solvent system(Wang et al. 2011). Although regenerated cellulose films have less crytallinity and polymeriztion degree than native cellulose, thery provides an opportunity to study cellulose degradation on model cellulose surface. Recently, the appearance of thin film of lignocellulosic nanofibrils (LCNFs) enables the modelling of cellulose hydrolysis on more representvative substrates for native cellulose. LCNF consist of crystalline cellulose I and amorphous region, which is present in fibrillar structure (Ahola et al. 2008a). Kumagai et al. (2013) have reported the application of LCNFs to study enzyme degradation monitored by QCM-D and found that the frequency changes in adsoption stage was different from the typical changes reported for pure cellulose.

The real-time meaurement of enzyme binding and hydrolysis by QCM-D also enables the modeling of enzymatic kinetics, which can be used to optimize the effects of various reaction conditions. The key for model development is to recongize that enzyme binding and hydrolysis contribute to the observed change in mass throughout the entire process. Some models have been reported to describe the interaction between cellulose film and cellulase successfully. Rojas group proposed an empirical model, which fit enzyme binding as an exponential decay function and described cellulose degradation with Boltzmann sigmoidal equation (Turon et al. 2008, Hu et al. 2009). By appling classic Michaelis-Menten model to continous flowing QCM system, Li (2012) successfully used the reaction steps to model the adsorption, hydrolysis and enzyme complex formation under various inhibitor (cellobiose) and enzyme concentrations. Also, Maurer (2012) proposed a kinetic model which combines Langmuir adsorption model and Michaelis-Menten activity of adsorbed enzyme to describe the competitive adsorption and cooperative activity of the mixture of cellobiohydrolase I (Cel7A) and endoglucanase I (Cel7B) from *T. longibrachiatum* meausured by QCM on 4MMO/DMSO cellulose films. A 1:2 bulk mass ratio of Cel7B : Cel7A is found to give optimum cellulose hydrolysis rate (Maurer et al. 2012, Maurer et al. 2013).

CHAPTER TWO

Activity and Distribution (Free and Cell-Bound) of Cellulosomes from *Clostridium thermocellum*

Summary

Clostridium thermocellum, a well-studied cellulolytic bacterium, produces highly active cellulases in the form of cellulosomes. The cellulolytic activity of *C. thermocellum* is greater than that of free fungal cellulase (Bayer et al. 2004). The ability of the cellulosome to adhere *C. thermocellum* cells to the cellulose substrate is considered to contribute to its high cellulose degradation activity. Although the synergy of having cell-attached cellulosomes is widely accepted, the relative importance of cell-bound and free cellulosomes on observed cellulose hydrolysis rates is unclear. In this study, a surface measurement technique, quartz crystal microbalance with dissipation (QCM-D), was used to examine the interactions between *C. thermocellum* and a model cellulose surface. To clearly differentiate the activity of free cellulosome and cell-bound cellulosome, the distribution of free cellulosome and cell-bound cellulosome in crude cell broth at different growth stages of *C.thermocellum* was quantified. For *C. thermocellum* strain ATCC 27405 in late exponential phase, greater than 70% of the cellulosome in the crude cell broth was shown to exist unattached to the cell. The hydrolysis of free cellulosome and crude cell broth measured by QCM on uniform amorphous (LiCl/DMAc dissolved) cellulose films indicated these two cellulase sources had significant initial hydrolysis rates, but different adsorbed "masses" on the film, potentially due to the differences in measuring by QCM the mass enzymes and cells adhered to the substrate. Furthermore, cellobiose inhibition of cellulase activity measured using Remazolbrilliant blue R dyed β-glucan (blue assay) suggested that the free cellulosome was more sensitive to cellobiose than the crude cell broth, which provides opportunities for further study on cellulose hydrolysis by *C.thermocellum* using QCM.

Introduction

Clostridium thermocellum is an anaerobic, cellulolytic, thermophilic, Gram-positive bacterium. It is capable of producing a large enzyme complex, termed a cellulosome, to degrade cellulose into cellodextrins, which are further fermented into

ethanol or other products by cells (Zhang and Lynd 2005). The ability of *C. thermocellum* to adhere to cellulosic substrates is well documented (Bayer et al. 1983, Dumitrache et al. 2013, Lynd et al. 2002). The adherence is believed to bring the cells close to the substrate and enable efficient uptake of hydrolysis products by the cells (Lynd et al. 2002). In fact, an adhesion-defective mutant of *C. thermocellum*, which was selected by enriching cells which failed to adhere to cellulose, has been reported to show reduced hydrolysis activity (Bayer et al. 1983). Furthermore, the adhesion of *C. thermocellum* is found to be mediated by the cellulosome, which is anchored to the cell via type II cohesion domain (Lynd et al. 2002), while the presence of cellulose binding modules within the cellulosome enables the binding of cell associated with cellulosome to cellulose (Shoham et al. 1999, Lynd et al. 2002, Bayer et al. 1983, Lamed et al. 1983). Supporting the possibility of enhanced hydrolysis efficiency in the presence of cell adherence to cellulose, recent work (Lu et al. 2006) has shown that the growing cultures of *C. thermocellum* (in which cell-bound cellulosome and cell-free cellulosome both exist) exhibited 2.3-4.5 fold higher hydrolysis ability than cell-free cellulosome.

The adherence of *C. thermocellum* to cellulose is a key factor in cellulose degradation and is mediated by cell-bound cellulosome. However, cellulosomes may exist in both cell-bound and extracellular forms. Early research (Bayer et al. 1985) has shown that cellulosomes are attached to the cell surface in the early exponential growth phase. The cell-bound cellulosome is then detached from cell surface as the life cycle goes on. By the stationary phase, most cellulosomes are in extracellular form (Demain et al. 2005, Bayer et al. 1998). Determining the state of the cellulosome (cell-bound cellulosome or cell-free cellulosome) is critical to the interpretation of the cellulolytic activity, as determined by cellulase assays or when extending the use of interfacial techniques to cellulases from whole cells.

As an advanced surface measurement technique, quartz crystal microbalance with dissipation (QCM-D) (Turon et al. 2008) has been successfully used for in situ and real time measurement of adsorption and hydrolysis of commercial fungal cellulase on model cellulose films. The application of QCM to cellulose degradation investigations presents the possibility of studying enzyme hydrolysis on cellulose substrate with various substrate properties(Ahola et al. 2008a), and examining the effect of other reaction conditions (pH, temperature, enzyme concentration) on hydrolysis kinetics. Various enzymatic kinetic models have also been developed based on real time measurement of QCM (Turon et al. 2008, Hu et al. 2009), with a goal of quantifying

the adsorption and hydrolysis steps for comparison across substrates and reaction conditions.

In the present work, a separation method for cell-bound cellulosome and free cellulosome was developed and the distribution of free cellulosome and cell-bound cellulosome in crude cell broth at different growth stages of *C.thermocellum* was quantified to clearly differentiate the activity of free cellulosome and cell-bound cellulosome. To examine the interactions between *C. thermocellum* and a model cellulose surfaces, quartz crystal microbalance with dissipation (QCM-D) was utilized to monitor in real time the hydrolysis of amorphous (LiCl/DMAc-solubilized) cellulose film by cellulases in a crude cell broth or free cellulosomes. Furthermore, inhibition of cellulase activity by cellobiose was measured using dyed β-glucan (blue assay) to study the sensitivity of the free and cell-bound cellulases of *C.thermocellum* to inhibition.

Materials and Methods

Materials: Microcrystalline cellulose (MCC, 20 μm) was supplied by Aldrich. D (+)-cellobiose (98%), ammonia (28-30 wt %), polyethyleneimine (PEI, 50 wt. % aqueous solution) were purchased from Acros Organics. Methanol (99.9%), N, N-dimethylacetamide (DMAc, 99.99%), lithium chloride (99.8%), hydrogen peroxide (30%), Tris buffer (0.3 M), glycerol (99.9%) were supplied by Fisher Scientific. Beta-glucazyme tablets (60 mg) were purchased from Megazyme (Ireland).

Source and maintenance of strains: *C.thermocellum* ATCC 27405 was used. Long term culture storage was prepared by anaerobically diluting 3 ml stock culture (late log phase) with 3ml of 50% deoxygenated glycerol and stored at -80ºC.

Medium and cultivation condition: The composition of Thermophile medium (T medium) per liter is: 1ml resazurin stock, 1.53g Na_2HPO_4, 1.5g KH_2PO_4, 0.5g NH_4Cl, 0.5g $(NH_4)_2SO_4$, 0.09g $MgCl_2·6H_2O$, 0.03g $CaCl_2$, 0.5g cysteine, 2.0g yeast extract, 10ml standard vitamins mixture, 5ml modified metal mixture (Pfennings metals plus 10mg $Na_2WO_4·2H_2O$ and 1mg Na_2SeO_3). The pH of the medium was adjusted to 6.7 with NaOH before being autoclaved at 121 ºC for 60 minutes to degas. Then the medium was bubbled with CO_2 until it cooled to room temperature, after which 50 ml 8% Na_2CO_3 (4g/50ml) was anaerobically added. Medium for batch culturing was

anaerobically transferred to serum bottles with Whatman No.1 filter paper (cellulose) and then autoclaved at 121 °C for 60 minutes for sterility. *C. thermocellum* was cultured anaerobically at 65 °C by routinely transferring 1 ml of cell culture to 9 ml T medium (10% inoculation) every two days (48 h). Finally, 1 ml of cell culture was transferred to 9 ml T medium with 4g/l cellobiose once to consume the residual cellulose before any further measurement by QCM (Fig.2.1).

Figure 2.1 *C. thermocellum* **culturing procedure**

Optical density measurement for bacteria population: The concentration of *C.thermocellum* was quantified by the absorbance reading at 600 nm of the cell broth measured by UV- vis spectrophotometer (8453, Agilent Technologies). T medium was used as a blank. The final reading was the average of three replications. Bacterial dry cell weights (DCW) were determined by optical density at 600 nm (OD_{600}). For *C.thermocellum*, one unit of OD_{600} was shown to correspond to 0.464 g DCW /L (Bothun 2004).

Separation of cellulosome fraction: Cells (and cell-attached cellulosomes) were removed from the crude cell cultures of *C. thermocellum* by centrifugation (3000 ×g for 20 min at room temperature (23°C)). The resulting supernatant was the free cellulosome fraction. The cell-bound cellulosome was obtained by resuspending the above-mentioned pellet in the T medium, which of same volume as the original broth.

To resuspend the pellet, the suspension was stirred vigorously on vortex mixer for 10 min. The separated fractions were imaged to examine separation efficiency (described below).

Lithium Chloride/Dimethylacetamide (LiCl/DMAc) cellulose film preparation: The preparation of cellulose film was adapted from a previous investigation (Notley et al. 2006, Eriksson et al. 2005). To make cellulose solution, firstly, 0.5 g microcrystalline cellulose (MCC) was immersed in 10 ml deionized water with continuous stirring for 24 h to allow the cellulose to swell and open the structure. After overnight stirring, most water of the suspension was removed by filtration. To exclude the residual water, the residue was immersed in 10 ml methanol with continuous stirring for 30 minutes, then filtered. This was repeated for three times. Methanol was removed by placing the residue in 10 ml N, N-dimethylacetamide (DMAc) with continuous stirring for 30 minutes then filtered, which was repeated for three times. This 0.5 g DMAc extracted cellulose was then added to 18 ml DMAc which was already heated to 150 °C. The activation process took place at 150 °C with refluxing DMAc for 30 minutes to opening polymer chains. After activation, the solution was cooled to 100 °C for 20 minutes. Then 1.5 g oven dried lithium chloride (LiCl) was added to dissolve cellulose substrate, after which the solution was left to cool to 25 °C with stirring overnight. Finally, a clear and colorless cellulose solution was obtained. 5 ml of this cellulose solution was further diluted with 20 ml DMAc to make 0.5% w/w cellulose solution, which was subsequently heated to 100 °C before spin-coating.

Prior to spin-coating with cellulose solution, the gold sensors (QSX 301, Q-sense, Göteborg, Sweden) were treated with ultraviolet cleaner (BioForce, Ames, IA) for 10 minutes to remove the organic contaminants on the sensor surface. The UV/ozone treated sensors were further cleaned in the 5:1:1 mixture of Milli-Q water, ammonia (25%), hydrogen peroxide (30%) at 75 °C for 5 minutes. After rinsing with deionized water to remove residual reagent, the sensors were dried with nitrogen gas and treated with UV/ozone again. The cleaned sensors were then placed in 2% w/v polyethyleneimine (PEI, 50 wt. % aqueous solution) solution for 10 minutes to coat the sensors with PEI, which is used as an anchoring polymer to help the cellulose attach to the sensor surface and stabilize in aqueous solution. The PEI treated sensors were rinsed with deionized water for 5 seconds and then water was removed by nitrogen gas. The polymer coated sensors were then dried in oven at 50 °C for 1 h. Finally, the sensors

were ready for spin-coating with cellulose solution. Heated cellulose solution 0.5% w/w (80 μl) was spin coated on the PEI coated sensor with the spin-coater (WS-400BZ-6NPP/Lite, Laurell Technologies) at 3000 rpm for 45 seconds. This was repeated three times. After spin-coating, the cellulose coated sensors were immersed in deionized water for 30 minutes to remove excess solvent (DMAc and LiCl), after which the water was removed with nitrogen and the cellulose film was dried in oven at 50 °C for 1h. The prepared cellulose films were stored in a desiccator at room temperature until use. The mass of cellulose coated on the sensor surface was measured by QCM-D.

***C. thermocellum* imaging on cellulose films:** Samples (crude cell broth, supernatant, pellet suspension) were placed dropwise on prepared LiCl/DMAc cellulose films and observed using a NIKON Eclipse 80i microscope (NIKON Instrument Inc.) at 20x magnification.

Cellulase activity assay: Remazolbrilliant blue R dyed β-glucan (blue assay) (McCleary 1991, McCleary and Shameer 1987) was used to compare the bulk activity of crude cell broth, free cellulosome and cell-bound cellulosome. The principle of the assay is that water soluble dyed fragments are produced when the dyed cellulose tablet is hydrolyzed. Increasing dyed fragments in solution are measured as increasing UV-vis absorbance at 590 nm, which can be related to enzyme activity. Test tubes (16×120 mm) with 0.5ml enzyme solution were incubated in a 60 °C water bath for 5 min. Following this, the reaction was initiated by adding a Beta-Glucazyme tablet (60 mg, Megazyme, Ireland). After exactly 10 min, 10 ml Trizma base solution (pH=8.5) was added to stop the reaction. To extract the dyed fragments, the content of the tubes was stirred vigorously on vortex mixer and allowed to stand at room temperature for about 5 min. This slurry was filtered using Whatman No.1 (9cm) filter paper (Fisher Scientific). The absorbance of filtrate at 590 nm was measured using a UV- vis spectrophotometer (8453, Agilent Technologies). The blank was prepared by adding 10 ml of Trizma base solution to the enzyme solution before adding the Beta-Glucazyme tablet. Three replicates were conducted.

QCM-D measurement of cellulose hydrolysis by C.thermocellum: The QCM-D (E4, Q-sense, Göteborg, Sweden) was used to measure the hydrolysis activity and binding of *C.thermocellum* on the LiCl/DMAc cellulose films. In a typical experiment, prior to

injection to the QCM module, all solutions (buffer and enzyme solution), which used T-medium (pH=6.7) as solvent, were placed in vacuum oven (285A, Fisher Scientific) at 50 °C for 1h to degas. Further degassing was performed at 50 °C in an ultra-sonicator (Cole-Parmer 8890, IL) for 20 minutes. The hydrolysis was conducted at 50 °C by controlling the QCM chamber at 50 °C and placing all solutions in a 50 °C water bath. After the temperature of chamber and solutions reached 50 °C, the degassed buffer solution was firstly introduced to QCM at a flow rate of 0.1 ml/min to let cellulose film fully swell and establish a stable baseline signal (Turon et al. 2008). When a constant frequency reading ($\Delta f < 2$ Hz/hr) was obtained, buffer solution was switched to enzyme solution (crude cell broth, free cellulosome, or cell-bound cellulosome). During this period, the frequency and dissipation of the thin film cellulose were monitored. When the frequency was not changing ($\Delta f < 2$ Hz/hr), buffer solution was injected for 30 minutes to rinse off the unbound cell and hydrolysis product on the sensor surface.

Result and Discussion

C.thermocellum **cultivation**

The cell culture was transferred to medium with crystalline cellulose (Whatman No.1 filter paper) regularly to maintain the extracellular organelle (cellulosome) that the cell uses to degrade cellulose. Cells were transferred to medium with 4 g/L cellobiose prior to QCM experiments for 28 h (stationary phase) to consume the residual cellulose, which could provide an undesirable background contribution to the frequency change observed in the QCM upon the introduction of the cellulase. Removing the residual cellobiose was not necessary, prior to the QCM measurements. The residual cellobiose in the cell broth at stationary phase was about 0.05g/l, as measured by HPLC, which indicates that cellobiose was almost completely consumed by the cell.

The optical density at 600nm (OD_{600nm}) of cell culture was taken hourly from inoculation (t=0 h) to monitor cell growth using cellobiose as carbon source. As shown in the growth curve (Fig.2.2), the cell had about 20 h growth lag. The cells grew rapidly once it entered log phase, and it took about 28 h to reach the stationary phase. This trends is consistent with literature (Johnson et al. 1989). Furthermore, the time to reach stationary phase using cellulose is about 48 h (data not shown) and for fructose is about 80h (Johnson et al. 1989). Thus, compared to cellulose and fructose, the growth on

cellobiose is relatively fast and cellobiose is the carbon source preferred by *C. thermocellum* (Lynd et al. 2002, Johnson et al. 1989). As observed, at about 28 h, the optical density reached a maximum and decreased slowly, which could be caused by greater cell death rate than cell growth rate due to lack of nutrients. The maximum optical density at 600 nm was about 1.20, corresponding to approximate 0.56 g dry cell weights/L as calculated from OD_{600} of $1.0 = 0.464$ g dry cell /L, as measured for *C. thermocellum* (Bothun 2004).
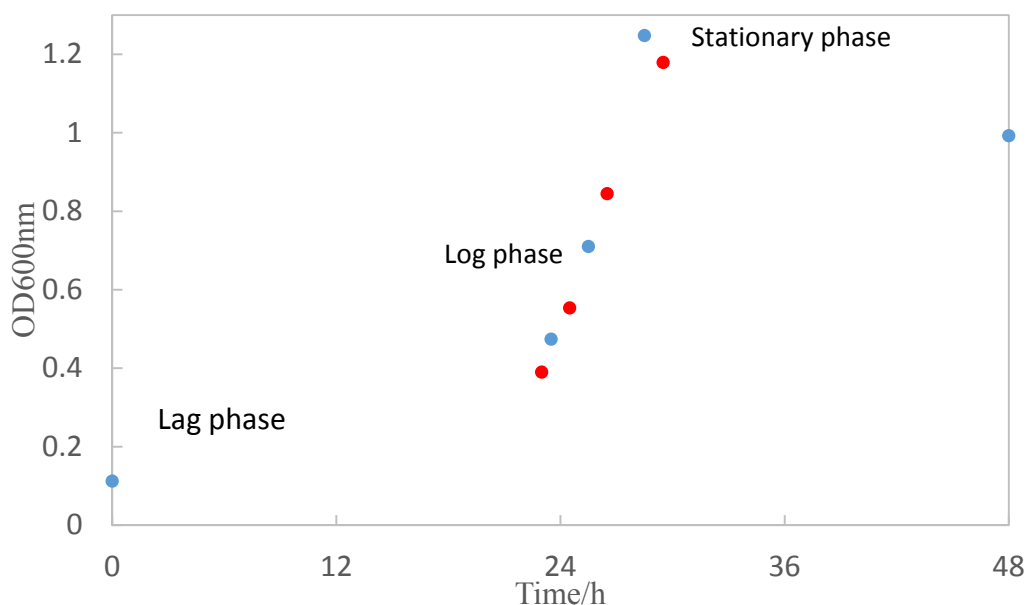
Figure 2.2 *C. thermocellum* **growth curve using cellobiose as carbon source**

Separation of free cellulosome and cell-bound cellulosome

A method to separate free cellulosome and cell-bound cellulosome was verified by varying the centrifuge speeds (centrifuge for 20 min). The corresponding optical density at 600 nm (OD_{600nm}) and optical microscopic images of supernatant (free cellulosome) and pellet suspension (cell-bound cellulosome) were used to select the centrifuge speed. Table 2.1 summarizes the optical density of the resulting supernatant and the resuspended cell pellet, and compares the total optical density to that of the original crude cell broth. As expected, the optical density of supernatant decreased and that of pellet suspension increased as the centrifuge speed increased, which indicates less cell residue in the supernatant and higher separation efficiency. The sum of the optical density of the supernatant and resuspended cell pellet at each centrifuge speed were similar to the optical density of the original crude cell broth ($OD = 0.756$). This suggests

that cells were recovered through suspending the pellet in medium, which justified this separation method for free cellulosome and cell-bound cellulosome.

Table 2.1 Optical density (OD$_{600nm}$) of supernatant and resuspended pellet suspension obtained after separation at various centrifuge speeds

Speed (×g)	original	200	600	1400	3000
Supernatant		0.566	0.161	0.040	0.014
Pellet suspension	----	0.176	0.619	0.755	0.751
Sum	0.756	0.742	0.780	0.795	0.765

The optical images of the model cellulose surface (Fig 2.3A) exposed to the supernatant and pellet suspension support the observations of cell density as a function of centrifuge speed. As shown for the crude cell broth on the cellulose surface (Fig 2.3 B), *C. thermocellum* has a rod shape approximately 20 - 50μm in length. This observation is consistent with other reports that cells are usually of 2 - 5μm in length (Freier et al. 1988, Bayer et al. 1985, Bayer and Lamed 1986, Bayer et al. 1994) and up to 40 μm is common under unfavorable conditions (Freier et al. 1988, Bayer et al. 1994). Meanwhile, the size of cellulosome complex is about 25 nm (Bayer et al. 1998). Thus, the cellulosome is not visible under the light microscopy. Compared to crude cell broth, fewer cells are observed in the supernatant and more cells are observed in the resuspended pellet with increasing centrifuge speed, which was consistent with the optical density result. Moreover, almost no cells in the supernatant were seen at speed of 3000 ×g (Fig 2.3 F (1)), which indicated that primarily free cellulosomes exist in the supernatant. This speed (3000 ×g) was used to separate free- and cell-bound cellulosomes for the remainder of the investigation.
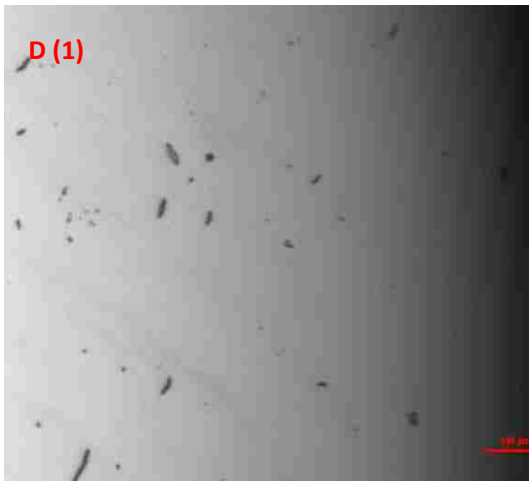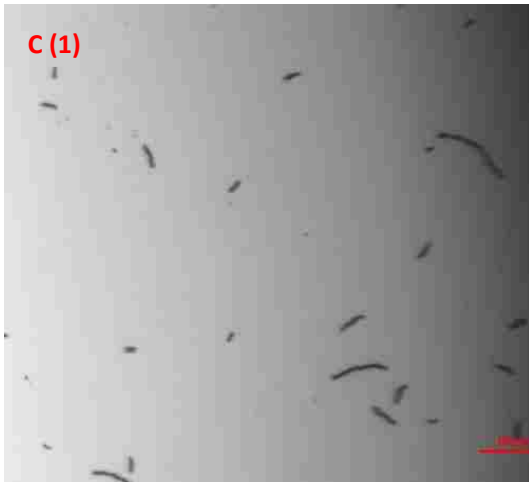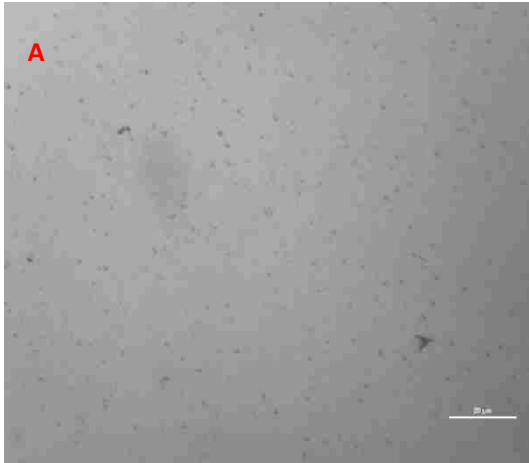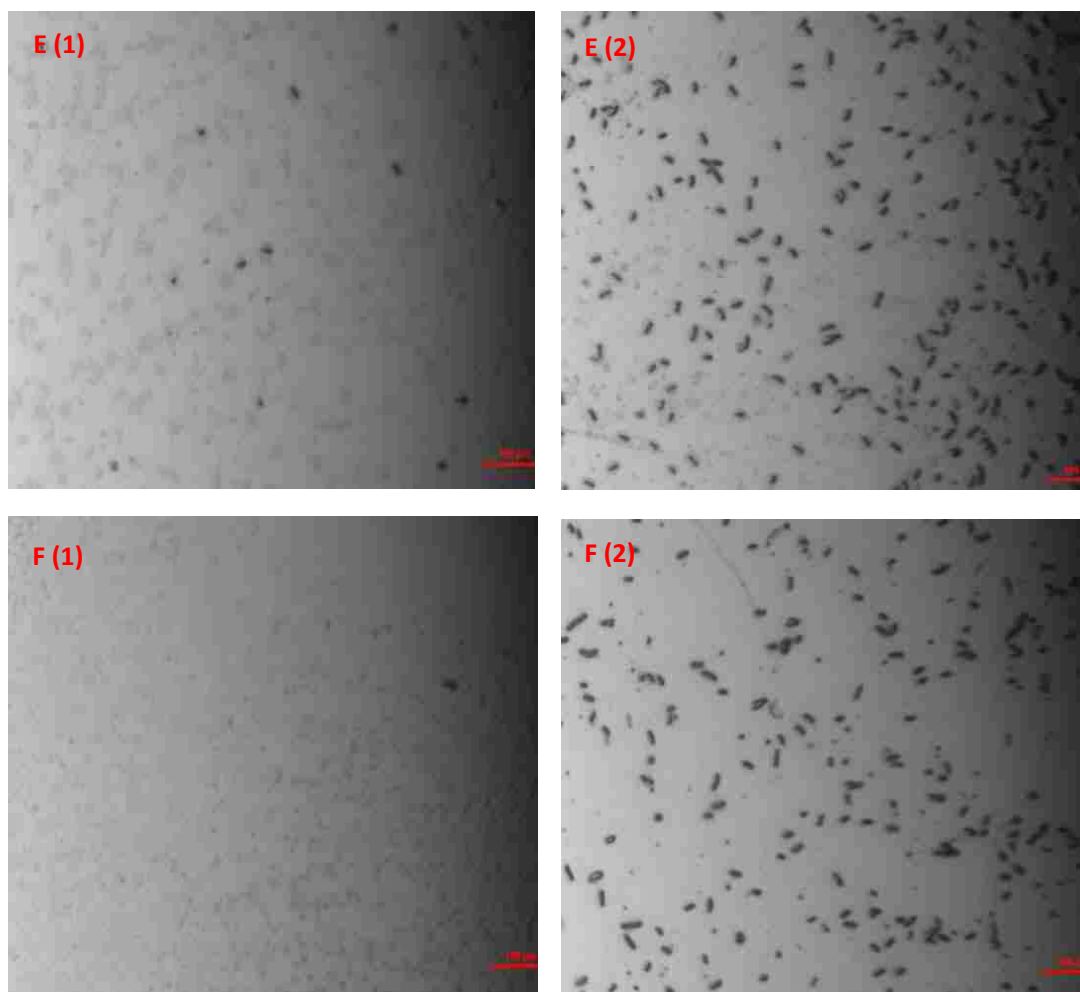
Figure 2.3 Supernatant (1) and pellet (2) suspension images obtained under various centrifuge speed: (A) cellulose surface, (B) 0 ×g (crude cell broth), (C) 200 ×g, (D) 600 ×g, (E) 1400 ×g, (F) 3000 ×g; Scale bar: 100µm.

Cellulosome distribution at different growth stages of *C. thermocellum*

To demonstrate whether cell-bound or free cellulosome is predominate in the cell broth at different growth stages, the activity of crude cell broth (free cellulosome and cell-bound both present), supernatant (free cellulosome) and pellet suspension (cell-bound cellulosome) at different growth stages (shown as red dots in Fig. 2.2) were measured by cellulase activity assay (blue assay) at 60 $^\circ$C. In the blue assay, dyed β-glucan is hydrolyzed by endo-acting cellulase and produces water soluble dyed fragments, resulting in increased absorbance at 590 nm (A_{590nm}). Therefore, cellulase activity can be quantified by the absorbance at 590 nm. Since all reaction conditions (pH, temperature, dyed β-glucan amount) were the same, higher A_{590nm} reading indicated higher hydrolysis activity and the presence of more active cellulosome.

As shown in Table 2.2, the activity of the three different fractions increased with the age of the cell culture, consistent with the presence of more cellulosome due to an increasing cell concentration. When normalizing the activity of free cellulosome and cell-bound cellulosome with the activity of crude cell broth, the sum of normalized activity of free cellulosome and cell-bound cellulosome was close to 1, indicating that the activity of the original crude cell broth was captured in the fractions of the supernatant and reconstituted cell pellet. The proportion of free cellulosome or cell-bound cellulosome relative to the total cellulosome is approximated by the corresponding normalized activity. It can be concluded that most cellulosome (> 70%) was in extracellular form at all growth stages.

Table 2.2 Cellulase activity as measured by the blue assay of crude cell broth, supernatant, pellet at different growth stages.

Growth stages		Early log phase	Mid log phase	Late log phase	Stationary phase
Growth time (h)		23	24.5	26.5	29.5
OD$_{600nm}$		0.390	0.553	0.844	1.179
Activity (A$_{590nm}$)	Crude cell broth	0.187	0.215	0.411	0.567
	Free cellulosome	0.145	0.184	0.295	0.487
	Cell-bound cellulosome	0.041	0.072	0.094	0.120
Normalized activity	Crude cell broth	1	1	1	1
	Free cellulosome	0.775	0.853	0.717	0.859
	Cell-bound cellulosome	0.219	0.337	0.229	0.212

In contrast, previous studies (Bayer et al. 1985, Mayer et al. 1987) demonstrate that most cellulosomes are attached to the cell surface in the early log phase and that they detach from the cell surface in the stationary phase, as monitored by electron microscopy using negative staining techniques for cellulosome visualization. Noteworthy is that the strain used in previous works was *C.thermocellum* YS or JW20 while the strain used in this study was ATCC 27405. Since the strain was evolving over decades, it is possible that properties are different between strains. Furthermore, it is

reported that a cellobiose-grown mutant (Bayer et al. 1983), which is selected by enriching cells which fail to adhere to cellulose, lacked cell-bound cellulosome (Bayer et al. 1985). The presence of this mutant also provides support for the appearance of less cell-bound cellulosome than free cellulosome in log phase in this study.

Hydrolysis activity of crude cell broth, free cellulosome and cell-bound cellulosome investigated by QCM

QCM-D was used to compare the binding and hydrolysis of crude cell broth, free cellulosome and cell-bound cellulosome obtained from stationary phase on amorphous cellulose thin film at 50 °C. A dramatic decrease in the frequency of the QCM occurs at 5 min (Fig.2.4 a), corresponding to the introduction of the crude cell broth, supernatant, or resuspended cell pellet into the QCM chamber. This frequency drop is interpreted as the binding of the cellulase to the cellulose surface. As the mass of the cellulose film decreased due to hydrolysis (observed as an increase in frequency) competes with the mass increase due to cellulase adsorption, a maximum frequency drop is observed. The frequency then continues to increase due to the cellulose mass loss by cellulase hydrolysis. As the substrate is consumed, the rate of frequency increase slows. This trend was observed for crude cell broth and free cellulosome, and has been observed previous for fungal cellulase (Turon et al. 2008). However, the hydrolysis rate, which can be represented by the slope of frequency changes following the minimum frequency, are quite different. Indeed, the crude cell broth showed highest hydrolysis ability, followed by the free cellulosome (supernatant), while the cell-bound cellulosome (resuspended pellet) didn't show significant hydrolysis activity.

The energy dissipation indicates the viscoelastic property change of cellulose film, which depends on the softness/rigidness of films (Schofield et al. 2007). As the enzyme introduced, the dissipation of crude cell broth and free cellulosome increase (Fig 2.4 b), indicating the formation of soft film due to the cellulase adsorption to the cellulose surface. A maximum dissipation value occurred and the dissipation started to decrease, as cellulose hydrolysis was dominant and resulted in a more rigid cellulose surface. This dissipation trend is similar to that of fungal cellulase as measured by QCM (Turon et al. 2008).

As shown in Fig.2.4 a, the crude cell broth showed greater hydrolysis activity but less maximum frequency drop than free cellulosome, which seems unreasonable since

crude cell broth have same amount of free cellulase as free cellulosome solution that should cause similar frequency drop. In fact, this observation is not contradict due to the existence of cell adsorption. Unlike cell-free cellulosome adsorption that can be interpreted by Sauerbrey equation in which the frequency drop is linearly with the bound mass, bacterial cell adhesion to substrate surface forms viscoelastic bacterium-substratum interface (Schofield et al. 2007) and makes the attached mass underestimate by Sauerbrey equation (Voinova et al. 2002, Olsson et al. 2009). Also, the dissipation of crude cell broth is always higher than that of free cellulosome (Fig.2.4 (b)) confirms the existence of a softer cellulose surface and a more viscoelastic interface in crude cell broth system. Therefore, the actual mass adsorbed of crude cell broth should be higher than the quantity calculated from Sauerbrey equation based on maximum frequency drop and comparable to the mass adsorbed of free cellulosome.

However, unlike crude cell broth and free cellulosome, the cell-bound cellulosome didn't show significant hydrolysis activity (Fig.2.4 a) and had constant increasing dissipation profile (Fig.2.4 b). Also, the cell-bound cellulosome didn't show a dramatic frequency drop at the time cellulase was introduced, which is usually seen on enzyme adsorption. Meanwhile, the images of cellulose film (Fig.2.5) after interacting with three cellulase fractions showed that cells were deposited on cellulose films uniformly, with cell-bound cellulosome (Fi2.5 D) showed more crowded cell deposition than crude cell broth (Fig.2.5 B) and the free cellulosome tended to distribute unevenly on the surface and build up as aggregates (Fig.2.5 C), which is visible under light microscopy. The accumulation of cells on cellulose surface is likely gravity driven. Therefore, the observed low hydrolysis activity of cell-bound cellulosome could result from that cells become inactive during the centrifugation and resuspending process and the frequency drop could just cause by cells which settle down on the cellulose surface under the effect of gravity.
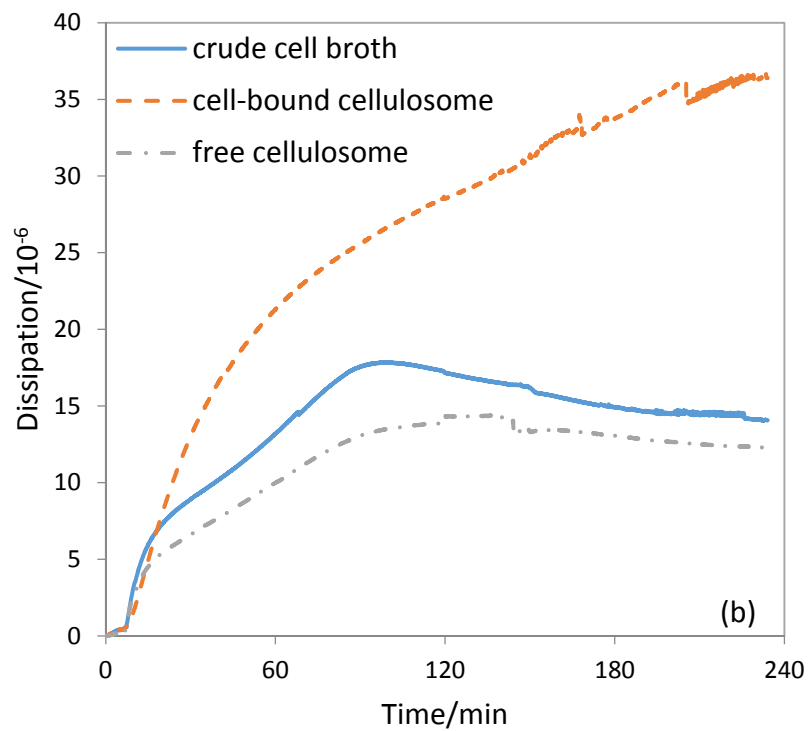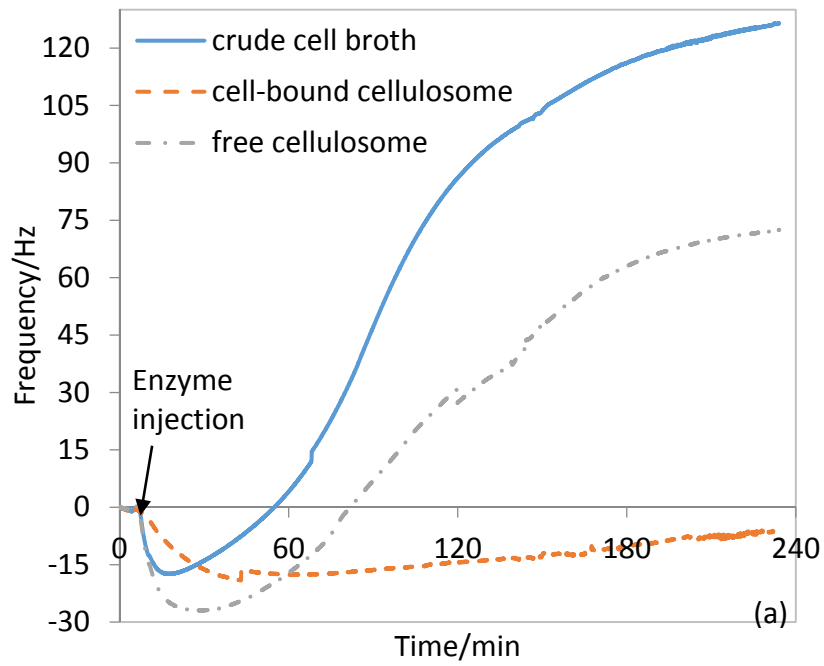
Figure 2.4 Frequency (a) and dissipation (b) profile of cellulose hydrolysis by crude cell broth, free cellulosome and cell-bound cellulosome obtained at 50 °C on an amorphous cellulose thin film.
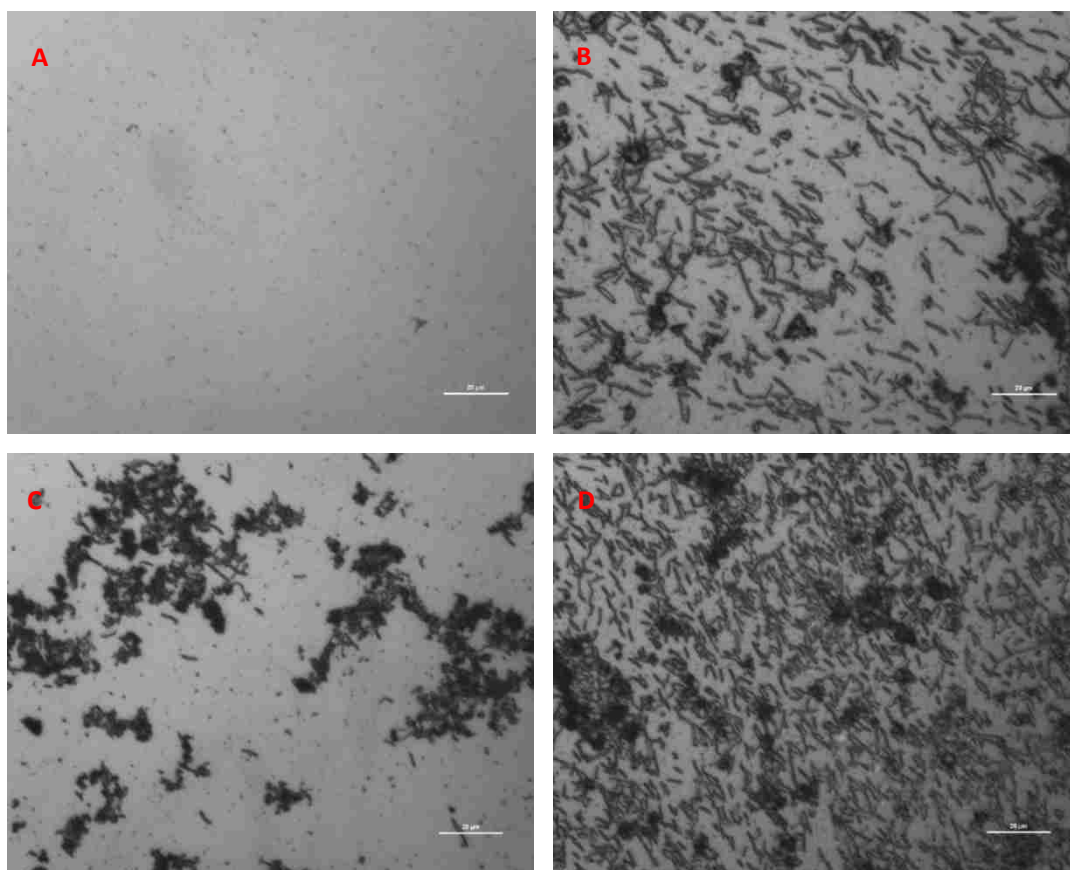
Figure 2.5 Images of cellulose surface after 240 min exposure time to the flow of cellulase solution in the QCM(A) crude cell broth (B), free cellulosome (C) and cell-bound cellulosome (D); scale bar: 20μm

Hydrolysis activity of crude cell broth, free cellulosome and cell-bound cellulosome measured by QCM and blue assay were also compared to demonstrate the difference between QCM and blue assay. As shown in table 2.3, the initial hydrolysis rates were the slope of QCM frequency changes following the minimum frequency and were normalized with the initial hydrolysis rate of crude cell broth. The sum of the normalized activity of free cellulosome (0.859) and cell-bound cellulosome (0.212) as measured by the blue assay was close to 1, suggesting that the cellulase activity of the blue assay is proportional to enzyme concentration. In contrast, the cellulase activity of the cell fractions measured by QCM does not appear to be additive. The difference may be influenced by the substrate. Dyed β-glucan is used in blue assay and the reaction occurs in the liquid phase, while cellulose film with certain degree of polymerization is used in QCM experiment and the interaction between cellulase and cellulose is a heterogeneous reaction. Thus, the reaction condition and substrate properties make cellulose more difficult to degrade in QCM experiment than the blue assay, causing

inconsistence in hydrolysis activity. Also, the experimental temperature for blue assay is 60ºC, which is the optimum temperature for cellulosome (Ng et al. 1977). However, QCM is conducted at 50 ºC due to experimental limitations of the technique. Thus, reaction temperature difference could also result in difference result in QCM and blue assay. In conclusion, QCM can be applied to study actual interaction between cellulosome and cellulose film under various condition such as pH, temperature and whole biomass substrates. Meanwhile, blue assay is more suitable for determining cellulosome distribution.

Table 2.3 Hydrolysis activity of crude cell broth, free cellulosome and cell-bound cellulosome measured by QCM and blue assay.

		Crude cell broth	Free cellulosome	Cell-bound cellulosome
Blue assay	Activity(A_{590nm})	0.567	0.487	0.120
	Normalized activity	1	0.859	0.212
QCM	Initial rate(Hz/min)	1.351	0.798	0.069
	Normalized activity	1	0.590	0.051

Cellobiose inhibition comparison between cell broth and free cellulosome at stationary phase

The activity of cell broth and free cellulosome obtained at stationary phase under various cellobiose concentration (0, 5, 10, 20, 30g/L) were measured by blue assay of cellulase activity. The reported activities at each cellobiose concentrations are normalized relative to uninhibited (0 g/L) cellobiose and summarized in Table 2.4. A graphical representation of cellulase activity as a function of cellobiose concentration is shown in Fig. 2.6. The cellulase activity decreased as cellobiose concentration increases. Complete inhibition is not observed even at the cellobiose concentration of 30 g/L. Furthermore, in the presence of the same concentration of cellobiose, the activity of free cellulosome was decreased more than the cell broth, which contained both free cellulosome and cell-bound cellulosome. Thus, the presence of cell-bound cellulosome could possibly reduce the inhibition effect of cellobiose.

Cellobiose, the dimer of cellulose and a product of cellulose hydrolysis, is a known inhibitor of cellulase activity (Johnson et al. 1982b). A cellobiose concentration of 20

g/L is reported (Lamed et al. 1985) to almost completely inhibit the activity of purified cellulosome from *C.thermocellum* YS with microcrystalline cellulose as substrate. Purified CelS (exo-glucanase), the most abundant catalytic subunit in cellulosome, and its activity is found to be 92% inhibited by cellobiose at 5 g/L using cellopentaose as substrate (Kruus et al. 1995), while purified endo-ß-glucanase of *C.thermocellum* is reported to be relatively insensitive to cellobiose when chromogenic substrate trinitrophenyl carboxymethyl-cellulose (TNP-CMC) was used as substrate (Johnson et al. 1982b). Thus, different catalytic units of the cellulosome have different sensitivity to cellobiose inhibition and the inhibition extent is strongly dependent on the substrate used (Johnson et al. 1982b). Since *C. thermocellum* strains are evolved over decades, the composition of catalytic units in cellulosome could differ from literature, which could lead to inconsistent inhibition concentration with literature when using different substrate.

Table 2.4 Cellobiose inhibition of crude cell broth and free cellulosome as measured by the blue assay of cellulase activity.

[Cellobiose]		0g/L	5g/L	10g/L	20g/L	30g/L
Crude Cell broth	Activity(A_{590})	0.567	0.557	0.608	0.523	0.473
	Normalized activity	1	0.984 ($\pm$0.023)	1.074 ($\pm$0.017)	0.922 ($\pm$0.023)	0.834 ($\pm$0.036)
Free cellulo-some	Activity(A_{590})	0.487	0.427	0.418	0.382	0.316
	Normalized activity	1	0.876 ($\pm$0.026)	0.857 ($\pm$0.020)	0.784 ($\pm$0.030)	0.649 ($\pm$0.026)
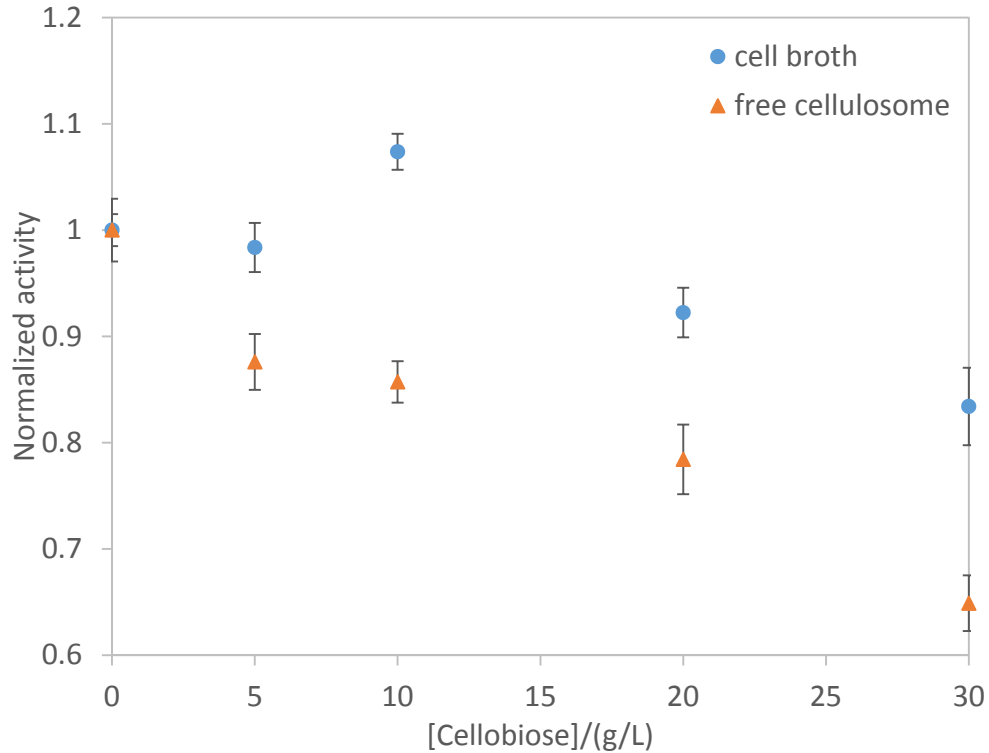
Figure 2.6 Cellobiose inhibition of crude cell broth and free cellulosome as measured by the blue assay of cellulase activity

Conclusion

To identify the relative importance of cell-bound and free cellulosomes on observed cellulose hydrolysis rates, a centrifuge-based separation technique is used to separate free cellulosome (supernatant) and cell-bound cellulosome (cell pellet) from crude cell broth. Using this separation technique, greater than 70% of the cellulosome in the crude cell broth is shown to exist unattached to the cell at all growth stages for strain ATCC 27405. Cellulase activity measurements in the presence of cellobiose suggest that free cellulosome is more sensitive to cellobiose inhibition than crude cell broth. Meanwhile, the hydrolysis activity of the crude broth can be captured from the activity of the free cellulosomes and the resuspended cells in the cellulase "blue" assay, but not from QCM measurements. However, QCM shows advantage over blue assay of cellulase activity for the study of the effect of reaction conditions on cellulose hydrolysis. The subsequent chapter uses QCM to investigate cellobiose inhibition on crude cell broth and free cellulosome, making use of the ability of this interfacial technique to examine the cellulosome/substrate interaction and the role cells plays in this interaction.

CHAPTER THREE

Quartz Crystal Microbalance Investigation of Inhibition of Crude Cell Broth and Free Cellulosome from *Clostridium thermocellum* by Cellobiose

Summary

Methods to examine the effect of reaction conditions on the enzymatic hydrolysis of cellulose at the interfacial level are needed to complement bulk cellulose hydrolysis experiments and guide the design of more efficient cellulose degradation processes. The conversion of cellulose into fermentable sugar by *C. thermocellum* and fungal cellulase is known to be inhibited by the end product cellobiose. Understanding the inhibition mechanism of cellobiose is particularly important for relieving product inhibition and improving cellulose hydrolysis efficiency. The quartz crystal microbalance with dissipation (QCM-D) has been successfully used to investigate the kinetics of cellulose hydrolysis by fungal cellulases in response to environmental perturbations, such as the presence of inhibitors. In this work, we extend the use of QCM-D to the measurement of cellulose hydrolysis by whole cell cellulases, specifically crude cell broth and free cellulosome from *C. thermocellum* (stationary phase) on amorphous cellulose films, under various cellobiose concentration (1, 3, 5, 10 g/L). The initial hydrolysis rates in the presence of crude cell broth or cell-free cellulosome decreased with increasing cellobiose concentration. Both crude cell broth and free cellulosomes had similar degrees of inhibition in the presence of cellobiose. At a concentration of 10 g/L cellobiose, the initial hydrolysis rate was reduced by approximately 74-79% relative to the uninhibited systems. The type of inhibition (competitive, noncompetitive, uncompetitive inhibition) can traditionally be interpreted from the initial hydrolysis rates as a function of inhibitor concentration. However, in these flow-through QCM experiments (constant enzyme and inhibitor concentrations) we demonstrated that the type of inhibition cannot be determined from initial rates. The similar inhibition patterns (within experimental concentration (0-10g/L)) observed for crude cell broth and free cellulosomes suggests that models developed for the cell-free cellulosomes, which allow for more accurate interfacial adsorption analysis by QCM than their cell-attached counterparts, may provide insight into hydrolysis events in both systems.

Introduction

Lignocellulose is the most abundant and sustainable biomass in nature, which makes it an attractive feedstock for biofuel production. However, the structure of lignocellulose, cellulose fibers wrapped by hemicellulose and lignin (Kumar et al. 2009), complicates the production of lignocellulosic biofuel. To solubilize the sugars needed to produce biofuel, lignocellulose is first pretreated to remove most lignin and hemicellulose to make the cellulose more accessible to cellulases. Cellulase then degrades cellulose to produce fermentable sugar through the synergistic action of at least three types of enzymes (Lynd et al. 2002). Exo-glucanase attacks crystalline cellulose chain ends to produce cellobiose, while endo-glucanase breaks down cellulose from the internal region (Xi et al. 2013). Cellobiose is further converted into glucose by ß-glucosidase. The sugar is fermented into biofuels by yeast or bacteria. The low efficiency of enzymatic hydrolysis of cellulose is the main cost barrier in economical lignocellulosic biofuel production. Therefore, improving cellulase activity is important for producing renewable, cost-competitive biofuels.

The factors affecting the enzymatic hydrolysis efficiency of cellulose include the cellulase source, the substrate (lignin content, crystalline degree etc.), reaction conditions (pH, temperature, enzyme concentration etc) and end-product inhibition (Sun and Cheng 2002). Pretreatment byproducts (organic acids, vanillin), intermediate hydrolysis products (cellobiose), and fermentation product (ethanol) are all cellulase inhibitors, which decrease the cellulase activity (Li 2012, Marju Gruno 2004).

Cellobiose is the main end-product of cellulose hydrolysis, and has been shown to strongly inhibit cellulase activity, leading to low conversion efficiency (Gusakov et al. 1985a, Holtzapple et al. 1990). Therefore, understanding the inhibition mechanism of cellobiose is particularly important for relieving product inhibition and improving cellulose hydrolysis efficiency. A challenge in measuring cellobiose inhibition from bulk reaction kinetics is that the hydrolysis rate quantified by the product formation rate can be inaccurate since the source of the hydrolysis product is both the substrate and the added inhibitor (Holtzapple et al. 1990, Teugjas and Valjamae 2013).

Quartz crystal microbalance with dissipation (QCM-D) allows the real time measurement of cellulase adsorption and substrate consumption, which offers opportunities for mechanistic studies of inhibition (Turon et al. 2008, Li 2012). Li (2012) has reported the use of QCM to study the interaction between fungal cellulase and semi-crystalline model cellulose films under various inhibitor and enzyme concentrations.

Fundamental models of cellulase adsorption, hydrolysis, and inhibition were applied to interpret the frequency response of the QCM data. In extending this investigation to cellulases from *C. thermocellum*, understanding the role of the cell in both the QCM frequency response and the observed hydrolysis rates is critical. However, bacterial cell are large colloidal particles, which will form viscoelastic bacterium-substratum interface if cells adheres to the substrate (Schofield et al. 2007). This non-rigidly attached mass has been shown to be underestimated by Sauerbrey equation in which the frequency drop is linearly with the bound mass (Voinova et al. 2002, Olsson et al. 2009). Moreover, there are examples that bacterial adhesion associated with positive frequency shifts (Olsson et al. 2011, Olsson et al. 2010). Therefore, unlike the adsorption of free cellulases (such as fungal cellulases), the frequency change of the QCM due to cell adsorption cannot be interpreted directly from the conventional mass-loading theory. The analysis of the dissipation term which describes the dissipative energy losses due to the viscoelastic behavior of the adsorbed mass is also needed to estimate the adsorbed mass (Olsson et al. 2011, Schofield et al. 2007).

The hydrolysis of amorphous cellulose films in the presence of crude cell broth and free cellulosome from *C. thermocellum* (stationary phase) was measured by QCM-D under various cellobiose concentration (1, 3, 5, 10g/L). The goal in comparing hydrolysis in the presence of different cell fraction was to examine the significance of cell adsorption on the measured response of the QCM in cellulose degradation studies and interpret interaction between *C.thermocellum* and the cellulose substrate. The kinetic models to interpret the mechanism of inhibition from the initial hydrolysis rate as a function of inhibitor concentration were extended from the traditional Michaelis-Menten approaches to the experimental flow system described by the QCM. The cellobiose inhibition pattern (0 – 10 g/L) of crude cell broth and free cellulosome were compared to examine the role that cell adherence plays in cellulosome/substrate interaction.

Materials and Methods

Materials: Microcrystalline cellulose (MCC, 20 μm) was supplied by Aldrich. D (+)-cellobiose (98%), ammonia (28-30 wt %), polyethyleneimine (PEI, 50 wt. % aqueous solution) were purchased from Acros Organics. Methanol (99.9%), N, N-dimethylacetamide (DMAc, 99.99%), lithium chloride (99.8%), hydrogen peroxide

(30%), Tris buffer (0.3 M), glycerol (99.9%) were supplied by Fisher Scientific. Beta-glucazyme tablets (60 mg) were purchased from Megazyme (Ireland).

Source and maintenance of strains: *C.thermocellum* ATCC 27405 was used. Long term culture storage was prepared by anaerobically diluting 3 ml stock culture (late log phase) with 3ml of 50% deoxygenated glycerol and stored at -80°C.

Medium and cultivation condition: The composition of Thermophile medium (T medium) per liter is: 1ml resazurin stock, 1.53g Na_2HPO_4, 1.5g KH_2PO_4, 0.5g NH_4Cl, 0.5g $(NH_4)_2SO_4$, 0.09g $MgCl_2\cdot6H_2O$, 0.03g $CaCl_2$, 0.5g cysteine, 2.0g yeast extract, 10ml standard vitamins mixture, 5ml modified metal mixture (Pfennings metals plus 10mg $Na_2WO_4\cdot2H_2O$ and 1mg Na_2SeO_3). The pH of the medium was adjusted to 6.7 with NaOH before being autoclaved at 121 °C for 60 minutes to degas. Then the medium was bubbled with CO_2 until it cooled to room temperature, after which 50ml 8% Na_2CO_3 (4g/50ml) was anaerobically added. Medium for batch culturing was anaerobically transferred to serum bottles with Whatman No.1 filter paper (cellulose) and then autoclaved at 121 °C for 60 minutes for sterility. *C. thermocellum* was cultured anaerobically at 65 °C by routinely transferring 1 ml of cell culture to 9 ml T medium (10% inoculation) every two days (48 h). Finally, 1 ml of cell culture was transferred to 9 ml T medium with 4g/l cellobiose once to consume the residual cellulose before any further measurement by QCM (Fig. 3.1).

Figure 3.1 *C. thermocellum* culturing procedure

Optical density measurement for bacteria population: The concentration of *C.thermocellum* was quantified by the absorbance reading at 600 nm of the cell broth measured by UV- vis spectrophotometer (8453, Agilent Technologies). T medium was used as a blank. The final reading was the average of three replications. Bacterial dry cell weights (DCW) were determined by optical density at 600 nm (OD_{600}). For *C.thermocellum*, one unit of OD_{600} was shown to correspond to 0.464 g DCW /L (Bothun 2004).

Separation of cellulosome fraction: Cells (and cell-attached cellulosomes) were removed from the crude cell cultures of *C. thermocellum* by centrifugation (3000 ×g for 20 min at room temperature (23°C)). The resulting supernatant was the free cellulosome fraction.

Cellulase activity assay: Remazolbrilliant blue R dyed β-glucan (blue assay) (McCleary 1991, McCleary and Shameer 1987) was used to compare the bulk activity of crude cell broth, free cellulosome and cell-bound cellulosome. The principle of the assay is that water soluble dyed fragments are produced when the dyed cellulose tablet is hydrolyzed. Increasing dyed fragments in solution are measured as increasing UV-vis absorbance at 590 nm, which can be related to enzyme activity. Test tubes (16×120

40

mm) with 0.5ml enzyme solution were incubated in a 60 °C water bath for 5 min. Following this, the reaction was initiated by adding a Beta-Glucazyme tablet (60 mg, Megazyme, Ireland). After exactly 10 min, 10 ml Trizma base solution (pH=8.5) was added to stop the reaction. To extract the dyed fragments, the content of the tubes was stirred vigorously on vortex mixer and allowed to stand at room temperature for about 5 min. This slurry was filtered using Whatman No.1 (9cm) filter paper (Fisher Scientific). The absorbance of filtrate at 590 nm was measured using UV- vis spectrophotometer (8453, Agilent Technologies). The blank was prepared by adding 10 ml of Trizma base solution to the enzyme solution before adding the Beta-Glucazyme tablet. Three replicates were conducted.

Lithium Chloride/Dimethylacetamide (LiCl/DMAc) cellulose film preparation:
The preparation of cellulose film was adapted from a previous investigation (Notley et al. 2006, Eriksson et al. 2005). To make cellulose solution, firstly, 0.5 g microcrystalline cellulose (MCC) was immersed in 10 ml deionized water with continuous stirring for 24 h to allow the cellulose to swell and open the structure. After overnight stirring, most water of the suspension was removed by filtration. To exclude the residual water, the residue was immersed in 10 ml methanol with continuous stirring for 30 minutes, then filtered. This was repeated for three times. Methanol was removed by placing the residue in 10 ml N, N-dimethylacetamide (DMAc) with continuous stirring for 30 minutes then filtered, which was repeated for three times. This 0.5 g DMAc extracted cellulose was then added to 18 ml DMAc which was already heated to 150 °C. The activation process took place at 150 °C with refluxing DMAc for 30 minutes to opening polymer chains. After activation, the solution was cooled to 100 °C for 20 minutes. Then 1.5 g oven dried lithium chloride (LiCl) was added to dissolve cellulose substrate, after which the solution was left to cool to 25 °C with stirring overnight. Finally, a clear and colorless cellulose solution was obtained. 5 ml of this cellulose solution was further diluted with 20 ml DMAc to make 0.5% w/w cellulose solution, which was subsequently heated to 100 °C before spin-coating.

Prior to spin-coating with cellulose solution, the gold sensors (QSX 301, Q-sense, Göteborg, Sweden) were treated with ultraviolet cleaner (BioForce, Ames, IA) for 10 minutes to remove the organic contaminants on the sensor surface. The UV/ozone treated sensors were further cleaned in the 5:1:1 mixture of Milli-Q water, ammonia (25%), hydrogen peroxide (30%) at 75 °C for 5 minutes. After rinsing with deionized

water to remove residual reagent, the sensors were dried with nitrogen gas and treated with UV/ozone again. The cleaned sensors were then placed in 2% w/v polyethyleneimine (PEI, 50 wt. % aqueous solution) solution for 10 minutes to coat the sensors with PEI, which is used as an anchoring polymer to help the cellulose attach to the sensor surface and stabilize in aqueous solution. The PEI treated sensors were rinsed with deionized water for 5 seconds and then water was removed by nitrogen gas. The polymer coated sensors were then dried in oven at 50 °C for 1 h. Finally, the sensors were ready for spin-coating with cellulose solution. Heated cellulose solution 0.5% w/w (80 μl) was spin coated on the PEI coated sensor with the spin-coater (WS-400BZ-6NPP/Lite, Laurell Technologies) at 3000 rpm for 45 seconds. This was repeated three times. After spin-coating, the cellulose coated sensors were immersed in deionized water for 30 minutes to remove excess solvent (DMAc and LiCl), after which the water was removed with nitrogen and the cellulose film was dried in oven at 50 °C for 1h. The prepared cellulose films were stored in a desiccator at room temperature until use. The mass of cellulose coated on the sensor surface was measured by QCM-D.

Atomic force microscopy (AFM) characterization on cellulose film：The surface morphology and roughness of cellulose film was measured by AFM (Series 4500, Agilent Technologies). The cellulose surface was scanned by silicon probes (TAP 300AI-G, Budget Sensors) with tip radius less than 10 nm in non-contact mode.

QCM measurements：The QCM-D (E4, Q-sense, Göteborg, Sweden) was used to measure the hydrolysis activity and binding of *C.thermocellum* on the LiCl/DMAc cellulose film. In a typical experiment, prior to injection to the QCM modules, all solutions (buffer and enzyme solution), which used T-medium (pH= 6.7) as solvent, were placed in vacuum oven (285A, Fisher Scientific) at 50 °C for 1 h to degas. Further degassing was performed at 50 °C in an ultra-sonicator (Cole-Parmer 8890, IL) for 20 minutes. The hydrolysis was conducted under 50 °C by controlling the QCM chamber at 50 °C and placing all solutions in a 50 °C water bath. After the temperature of chamber and solutions reached 50 °C, the degassed buffer solution (medium with 0 g/L, 1 g/L, 3 g/L, 5 g/L, 10 g/L cellobiose) was firstly introduced to QCM at a flow rate of 0.2 ml/min to let cellulose film to fully swell and produce a steady baseline QCM signal (Turon et al. 2008). When a constant frequency reading ($\Delta f< 2Hz/hr$) was obtained,

buffer solution was switched to enzyme solution (crude cell broth or free cellulosome with 0 g/L 1g/L, 3 g/L, 5 g/L, 10 g/L cellobiose). During this period, the frequency and dissipation of the thin film cellulose were monitored. When the frequency was not changing ($\Delta f < 2$ Hz/hr), the buffer solution was injected to rinse off the unbound cell and hydrolysis product on the sensor surface for 30 minutes.

Result and discussion

Lithium Chloride/Dimethylacetamide (LiCl/DMAc) cellulose film characterization

AFM in non-contact mode was used to measure the topography of the prepared cellulose films (Fig.3.2). The AFM images showed that the LiCl/DMAc films had a uniform structured feature in the micrometer scale, exhibiting non-fibrillar structure without any preferential orientation, which is consistent with the observations reported in the literature (Aulin et al. 2009, Eriksson et al. 2005). As reported in the literature, small incidence angle X-ray diffraction measurement also indicate that LiCl/DMAc films are amorphous cellulose substrate (Aulin et al. 2009). The conversion of crystalline cellulose to amorphous cellulose happens during the dissolution of cellulose in LiCl/DMAc solvent system. The LiCl/DMAc complex enters in competitive hydrogen bond formation with the hydroxyl protons of cellulose, which break the intermolecular hydrogen bonds linking the cellulose chains (McCormick et al. 1985, Morgenstern and Kammer 1996, Dupont 2003). The disorder of hydrogen bonds leads to formation of amorphous structure.
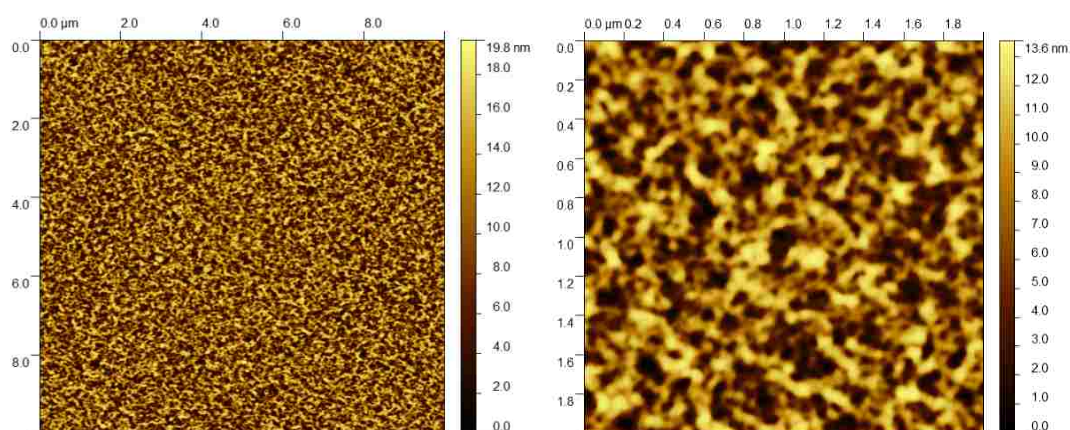
Figure 3.2 AFM images of cellulose film formed from dissolution in LiCl/DMAc: 10µm x 10µm (left), 2µm x 2µm (right).

The properties of cellulose films are of paramount importance in studying

enzyme/cellulose interaction. The chemical composition (lignin, hemicellulose percentage), surface morphology (accessible surface area etc), and substrate structure (crystallinity, degree of polymerization etc.) all affect the efficiency of cellulase hydrolysis (Turon et al. 2008, Ahola et al. 2008b). Model cellulose films can be prepared by spin-coating (Notley et al. 2006) or Langmuir-Blodgett deposition (Holmberg et al. 1997) of cellulose nanocrystal suspension, native cellulose microfibrils (MFC) suspension or regenerated cellulose solution on solid substrate, which result in cellulose films with different crystallinities (Aulin et al. 2009, Ahola et al. 2008b). Although cellulose films that can more closely mimic native cellulose is more desirable for some applications, cellulose films with high crystallinity often exhibit fibrillar structure and heterogeneous deposition (Aulin et al. 2009). A homogenous cellulose films instead can ensure consistent experimental measurements, which is important for comparison across hydrolysis conditions and modeling efforts. In order to decrease the complexity and reveal the role of cellulases plays in the cellulose hydrolysis regardless of substrate properties, regenerated cellulose dissolved in LiCl/DMAc is used in this work to prepare smooth amorphous cellulose model surfaces.

Effect of cellobiose (inhibitor) concentration on QCM response

The effect of cellobiose concentration on the frequency response of the QCM-D was investigated to quantify its contribution in subsequent hydrolysis experiment in the presence of the enzymes. Solutes such as cellobiose can change the observed frequency response due to adsorption to the thin film sensor or changes in the solution viscosity (Itoh and Ichihashi 2008, Martin et al. 1993). The measurements used a buffer solution (0 g/L cellobiose) to obtain base line (F = 0 Hz), after which buffer solutions with different cellobiose concentrations were injected (at t of approximately 10 min). Fig.3.3 shows that the injection of cellobiose solution (5, 10, 20, 30 g/L) resulted in 5.6, 7.3, 13.1, 25.1 Hz frequency drop (third overtone), respectively and an increase in energy dissipation, which indicates changes in the viscoelasticity and morphology of the film. Furthermore, the frequency drops were almost proportional to the cellobiose concentration (Fig. 3.4), which was caused by viscosity change of the solution adjacent to the film or the adsorption of cellobiose on the cellulose substrate. When cellobiose solution (5, 10, 20, 30 g/L) was switched to buffer solution (0 g/L cellobiose), the

frequency returned to the baseline with a slight offset (4.2, 3.4, 2.5, 1.6 Hz, respectively). This observation indicates that cellobiose is not irreversibly bound to the cellulose substrate and only small amount of cellobiose is bound to the cellulose film after rinsing (maximally causing a 4.2 Hz frequency drop in the experimental range of cellobiose concentrations). This offset represents a minimum change in frequency relative to the frequency change during hydrolysis (~100Hz), which is neglectable comparing to the mass loss of cellulose during hydrolysis. The potential for cellobiose to alter the observed changes in the frequency was addressed by equilibrating cellulose film with buffer which has the same cellobiose concentration as the enzyme solution before cellulose hydrolysis.
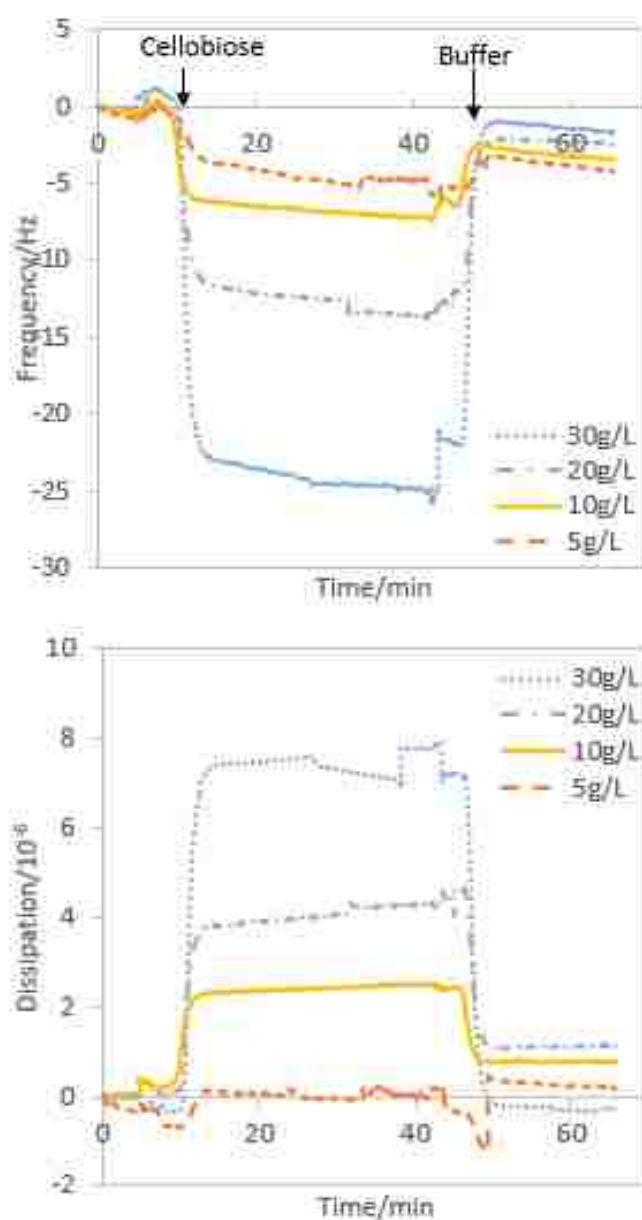
Figure 3.3 Frequency and dissipation profile of cellobiose loading at 50°C.
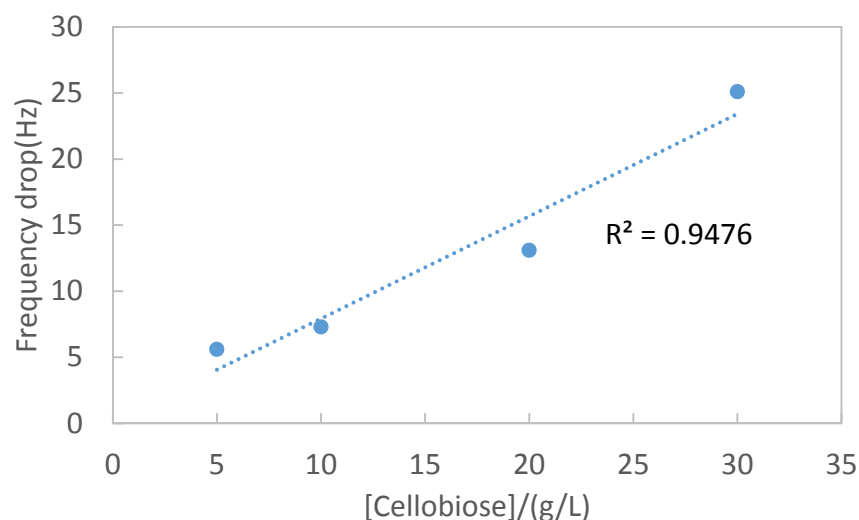
Figure 3.4 Maximum frequency drop of the cellulose-coated QCM sensor as a function of cellobiose concentration

QCM Measurement：cellobiose inhibition study on crude cell broth

Crude cell broth of *C.thermocellum* at stationary phase was added with cellobiose (0, 1, 3, 5, 10 g/L) to study the cellobiose inhibition effect on the hydrolysis activity for this mixture of cell-bound and free cellulosome. In order to offset any deviations caused by differences in cell density, a blank control that used the same cell broth in the absence of cellobiose (0 g/L) was conducted with each cellobiose inhibition experiment (1, 3, 5, 10 g/L). The frequency profiles for each cellobiose concentration are shown in Fig. 3.5.

Similar to the cellulose hydrolysis in the absence of cellobiose, the introduction of the inhibited crude cell broth into the QCM chamber at approximately 8 min leads to a dramatic decrease in the frequency due to the binding of the cellulase to the cellulose surface. As the mass loss of the cellulose film due to hydrolysis (observed as an increase in frequency), begins to compete with the mass increase due to cellulase adsorption, a maximum frequency drop is observed. For each cellobiose concentration, the difference between the maximum frequency drop of the uninhibited (0 g/L) and inhibited cell broth (1, 3, 5, 10 g/L) is 2.3, 5.6, 5.0 and -1.5 Hz, respectively, which doesn't show obvious relationship with cellobiose concentration. The interpretation of maximum frequency drop can be complicated since it represents the combined effect of cellulase adsorption and cellulose hydrolysis, while hydrolysis rate is also affected by cellobiose concentration. On the other hand, this complication reflects the potential of this interfacial technique to examine both adsorption and hydrolysis simultaneously.

Mechanistic models of enzyme kinetics can be tested and parameterized using the QCM frequency profile, where the successful prediction of the maximum frequency drop provides a stringent test of the proposed model.
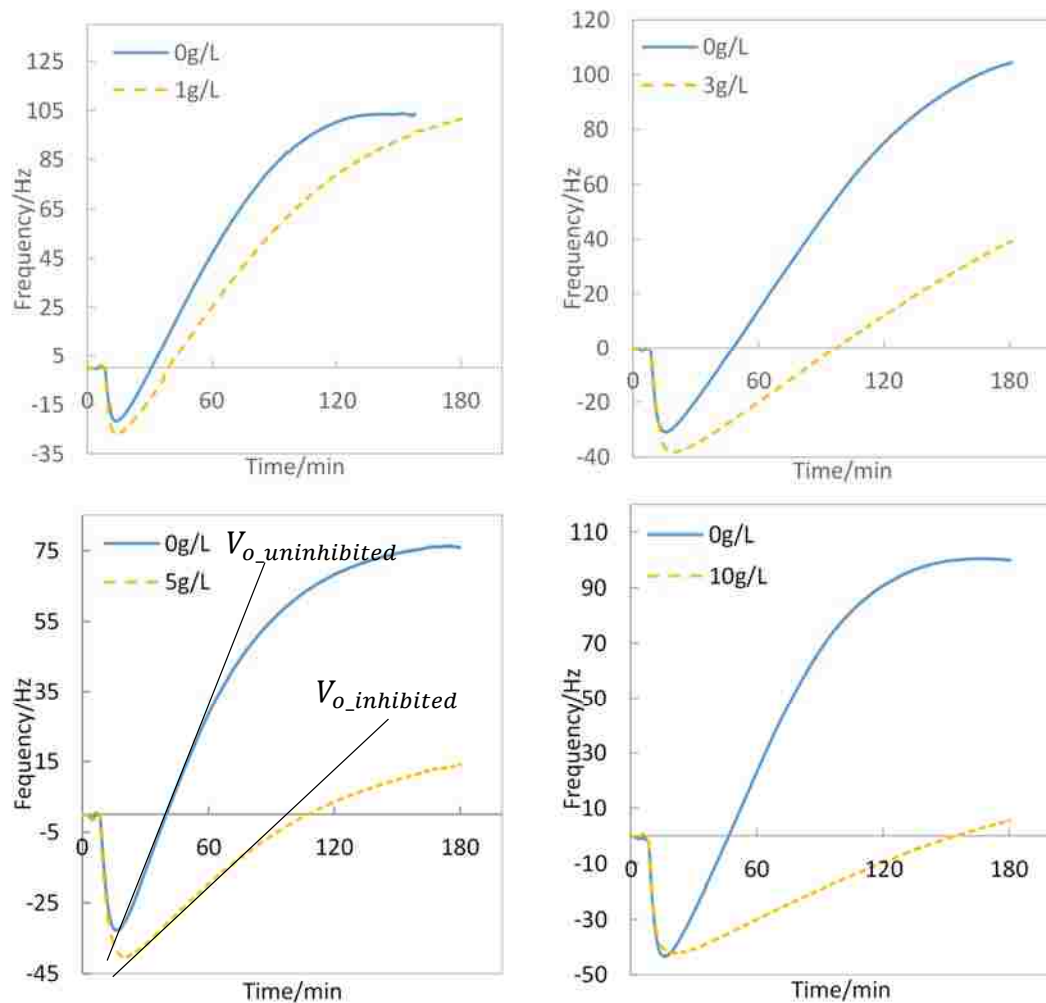
Figure 3.5 Frequency profile of cellulose hydrolysis by crude cell broth of *C.thermocellum* in the presence of cellobiose (1, 3, 5, 10 g/L) at 50 ºC on amorphous cellulose film.

The hydrolysis activity of cellulases can be quantified by initial hydrolysis rate (V_o), which is the maximum slope of the frequency curve after the minimum frequency (Fig.3.5). The initial hydrolysis rate of crude cell broth in the presence of cellobiose ($V_{o\_inhibited}$) and the corresponding initial hydrolysis rate in absence of cellobiose ($V_{o\_uninhibited}$) is summarized in Table 3.1. The extent of inhibition can be evaluated by normalizing $V_{o\_inhibited}$ by the corresponding $V_{o\_uninhibited}$, which eliminates effect of cell density differences. As shown in Fig. 3.7, inhibition of the initial hydrolysis rate

increases almost linearly with the cellobiose concentration for cellobiose concentrations less than 3 g/L. At higher cellobiose concentration, the inhibition extent is increasing but in a relatively slow rate. Within experiment condition (0 – 10 g/L), the highest extent of inhibition is 79%, observed at 10 g/L cellobiose.

Similar cellobiose inhibition study have been performed by Li (2012) using QCM-D, but fungal cellulase (0.5 % v/v) from *Trichoderma reesei* was used to degrade NMMO (semi-crystalline) cellulose films. In this work amorphous cellulose film (LiCl/DMAc) was chose as model cellulose film for studying activity of cellulosome from *C.thermocellum*. To compare the cellulase activity between *C.thermocellum* and fungal cellulase, similar processing was done on Li's data (Fig. 3.7). Fungal cellulase showed higher sensitivity to cellobiose than *C.thermocellum* and the activity was completely inhibited at 5 g/L. Moreover, as measured by blue assay, the activity of fungal cellulase (0.5 % v/v) crude cell broth of *C.thermocellum* (stationary phase) is 0.850 and 0.333, respectively. This doesn't necessary indicate that fungal cellulase has higher activity since the enzyme concentration in both system are not equivalent. Also, NMMO cellulose films and LiCl /DMAc cellulose films have different cellulose structures. Therefore, equivalent cellulase concentration and similar substrate are required to obtain more precise comparison between fungal cellulase and *C.thermocellum.*

Reversible enzymatic inhibition can be generally divided into three types: competitive inhibition, noncompetitive inhibition, uncompetitive inhibition. For example, *T. reesei* have been reported to be competitive and noncompetitive inhibited by cellobiose when the substrate were Avicel and rice straw, respectively(Holtzapple et al. 1990). Traditionally, Michaelis-Menten models are used to interpret kinetic data and determine the inhibition types by describing the hydrolysis rate expression in the form of double-reciprocal plots (a plot of the reciprocal of the observed hydrolysis rate against the reciprocal of the substrate concentration), which show distinguishable features for different inhibition types as a function of inhibitor concentration (Lineweaver and Burk 1934). However, the Michaelis-Menten model is developed under homogenous reaction conditions (Michaelis and Menten 1913). Thus it can't be directly applied to the hydrolysis of cellulose, which is a heterogeneous surface reaction. To interpret the cellobiose inhibition mechanism, modified Michaelis-Menten models for a continuous flow system (QCM system) were developed for three known inhibition mechanism (see Appendix A). The three inhibition types are shown to have similar

hydrolysis rate expression that is proportional to the cellobiose concentration (Eq.3.1-3.3) and predict the experiment data well (Fig.3.6). Therefore, the initial hydrolysis rate is not sufficient to determine the inhibition type.

$$\text{Competitive inhibition: } \frac{1}{v_{0\_inhibitied}} - \frac{1}{v_{0uninhibitied}} = \frac{K_m/[E_0]}{k_2 K_I \ [S_0]}[I] \quad (3.1)$$

$$\text{Noncompetitive inhibition: } \frac{1}{v_{0\_inhibitied}} - \frac{1}{v_{0uninhibitied}} = \frac{(1+\frac{K_m}{[E_0]})}{k_2 K_I [S_0]}[I] \quad (3.2)$$

$$\text{Uncompetitive inhibition: } \frac{1}{v_{0\_inhibitied}} - \frac{1}{v_{0uninhibitied}} = \frac{1}{k_2 K_I [S_0]}[I] \quad (3.3)$$
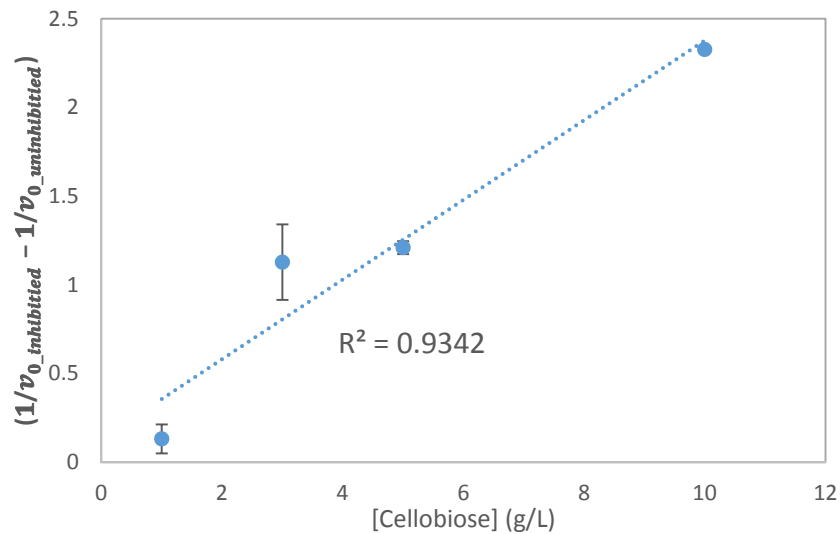
Figure 3.6 Cellobiose inhibited initial hydrolysis rate of crude cell broth of *C.thermocellum* as a function of cellobiose concentration (1, 3, 5, 10 g/L) at 50 ºC on amorphous cellulose film.

To further investigate the inhibition mechanism, fitting the interfacial models of inhibition described by the Michaelis-Menten equations to the entire frequency response, and not just the initial rates, would be required. Li (2012) applied mechanistic models to fit the QCM frequency profile to reaction steps of cellulase adsorption, inhibitor adsorption, inhibited enzyme adsorption, and cellulose hydrolysis for a system of *T. reesei* cellulase on NMMO cellulose film in the presence of cellobiose. Li investigated competitive, non-competitive and reactive enzyme-substrate-inhibitor (ESI) complex inhibition models, which proved to be unable to describe the experiment data. An inhibition model that combined competitive and non-competitive inhibition was proposed, which to best predict the frequency profiles as a function of inhibitor concentration. Li's work suggests the direct interpretation of the inhibition mechanism from the QCM frequency response. However, the contribution of attached whole cells

to the observed decrease in frequency is less quantifiable (Voinova et al. 2002, Olsson et al. 2009) and would need to be addressed further before model that includes whole cell adsorption to the cellulose surface could be validated.

Table 3.1 Summary of the initial rates of hydrolysis (V_o) for crude cell broths in the presence of cellobiose (three replications). Values are normalized relative to the initial rates for uninhibited (0 g/L cellobiose) experiments conducted using the same crude cell broth.

[cellobiose]	1g/L	3g/L	5g/L	10g/L
Optical density$_{600nm}$	1.32	1.19	1.39	1.39
$V_{o\_uninhibited}$(Hz/min)	1.568	1.219	1.415	1.626
$V_{o\_inhibited}$(Hz/min)	1.175	0.522	0.536	0.34
Normalized Hydrolysis Rate ($V_{o\_inhibited}$/$V_{o\_uninhibited}$)	0.749 (±0.089)	0.428 (±0.074)	0.379 (±0.016)	0.209 (±0.000)
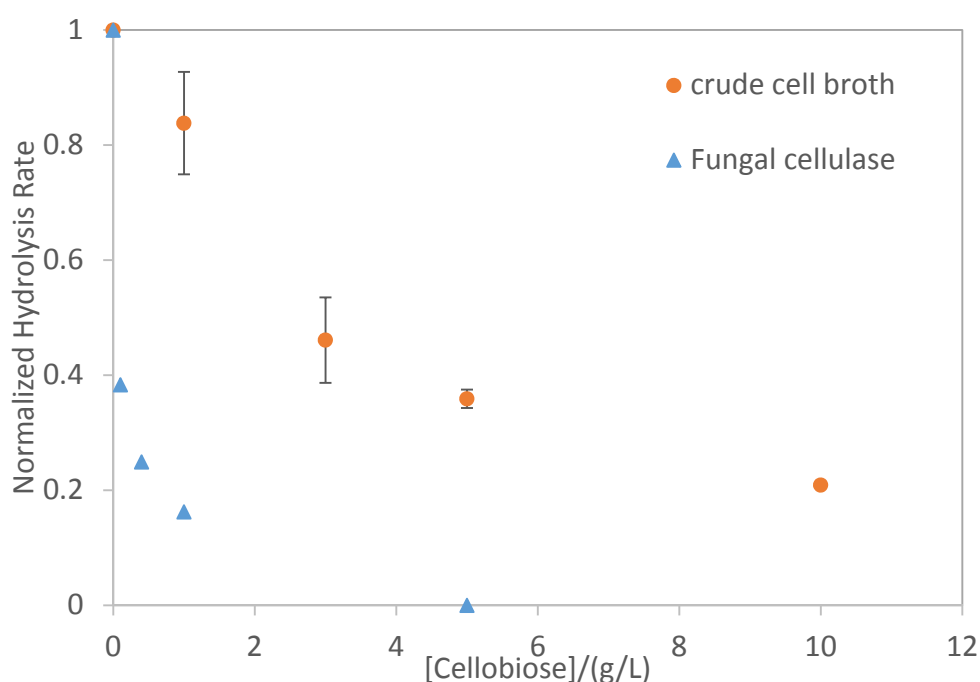
Figure 3.7 The normalized activity of crude cell broth of *C. thermocellum* and fungal cellulase (data adapted from Li (2012)) as a function of cellobiose concentration

QCM Measurement：cellobiose inhibition study on free cellulosome

The activity of crude cell broth and free cellulosome in the presence of cellobiose was compared to investigate the role of the cell in the observed inhibition. The effect of cellobiose on the activity of free cellulosome, obtained from supernatant of the crude *C.thermocellum* cell broth at stationary phase, was studied at cellobiose concentrations of (0, 1, 3, 5, 10g/L). A control that used the same free cellulosome solution but without the presence of cellobiose (0g/L) was conducted with each cellobiose inhibition experiment (1, 3, 5, 10g/L) to compensate for differences caused by cell density . The frequency profiles for each cellobiose concentration are shown in Fig. 3.8. The initial hydrolysis rate of free cellulosome in the presence of cellobiose ($V_{o\_inhibited}$) and corresponding initial hydrolysis rate in absence of cellobiose ($V_{o\_uninhibited}$) is summarized in Table 3.2.
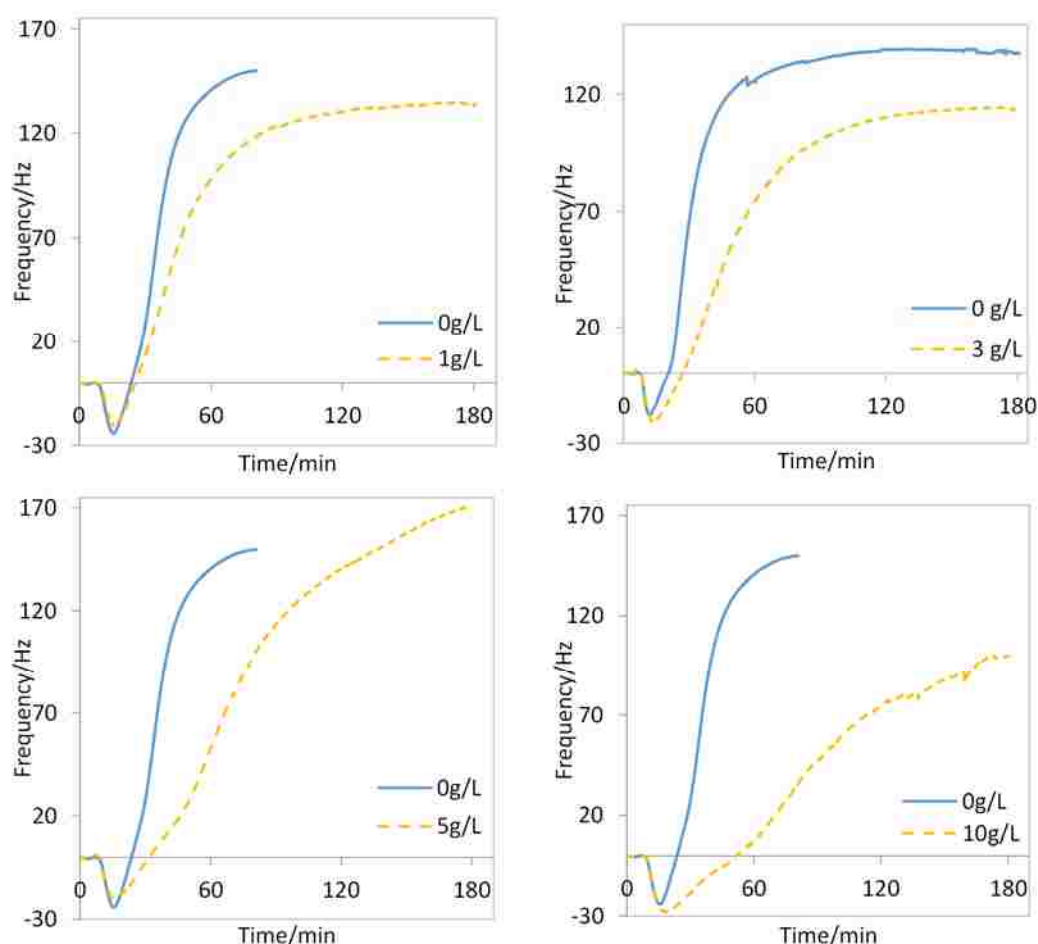
Figure 3.8 Frequency profile of cellulose hydrolysis by free cellulosome of *C.thermocellum* in the presence of cellobiose (1, 3, 5, 10 g/L) at 50 ºC on amorphous cellulose film.

51

The trends in QCM frequency in the presence of free cellulosomes was similar to that of crude cell broth, but free cellulosomes (V_o of approximately 3.7 Hz/min) was more active than crude cell broth (V_o of approximately 1.3 Hz/min) due to differences in the batch cell cultures. This difference is eliminated by normalizing the inhibited initial rate with the uninhibited initial rate, which allows comparison of the inhibition pattern. As shown in Fig. 3.9, cellobiose has a similar effect on the initial rate of hydrolysis for free cellulosome and crude cell broth. Johnson et al. (1982b) also reported that the free cellulosome and crude cell broth of *C. thermocellum* ATCC 27405 had similar cellobiose inhibition patterns on the substrates of phosphoric acid-swollen Avicel and microcrystalline Avicel. Furthermore, cellobiose does not affect the adherence of *C. thermocellum* to cellulose substrate (Bayer et al. 1983). The observation that crude cell broth and free cellulosome are affected similar by cellobiose suggests that mechanistic models of inhibition of the free cellulosome may be applied to understand inhibition in the crude cell broth, which contains both free cellulosomes and cell bound cellulosomes.

In this work, at a concentration of 10 g/L, about 74% inhibition is observed for cell-free cellulosomes as measured by QCM on amorphous cellulose film. However, the cellobiose inhibition measured by blue assay using β-glucan as substrate (Chapter 2) is only about 35% inhibition, is seen at a concentration of 30g/L. Furthermore, Johnson et al. (1982b) found that at 50 g/L of cellobiose the crude cell broth and free cellulosome of *C.thermocellum* was inhibited by 50% for phosphoric acid-swollen Avicel, while complete inhibition occurred at 20 g/L cellobiose with microcrystalline Avicel as substrate. Thus, cellobiose inhibition of *C. thermocellum* is strongly dependent on substrate structure. Furthermore, substrates that are easier to degrade tend to be less inhibited; β-glucan is easier to degrade than amorphous cellulose film and phosphoric acid-swollen Avicel is easier to degrade than microcrystalline Avicel. *T. reesei* is also found to have the same characteristic (Gruno et al. 2004).

Table 3.2 Summary of the initial hydrolysis rates and normalized rates of amorphous cellulose by free cellulosomes in the presence of cellobiose

[cellobiose]	1g/L	3g/L	5g/L	10g/L
$V_{o\_uninhibited}$(Hz/min)	3.778	3.624	3.778	3.778
$V_{o\_inhibited}$(Hz/min)	3.343	1.764	1.493	0.996
Normalized hydrolysis rate ($V_{o\_inhibited}/V_{o\_uninhibited}$)	0.885	0.487	0.395	0.263
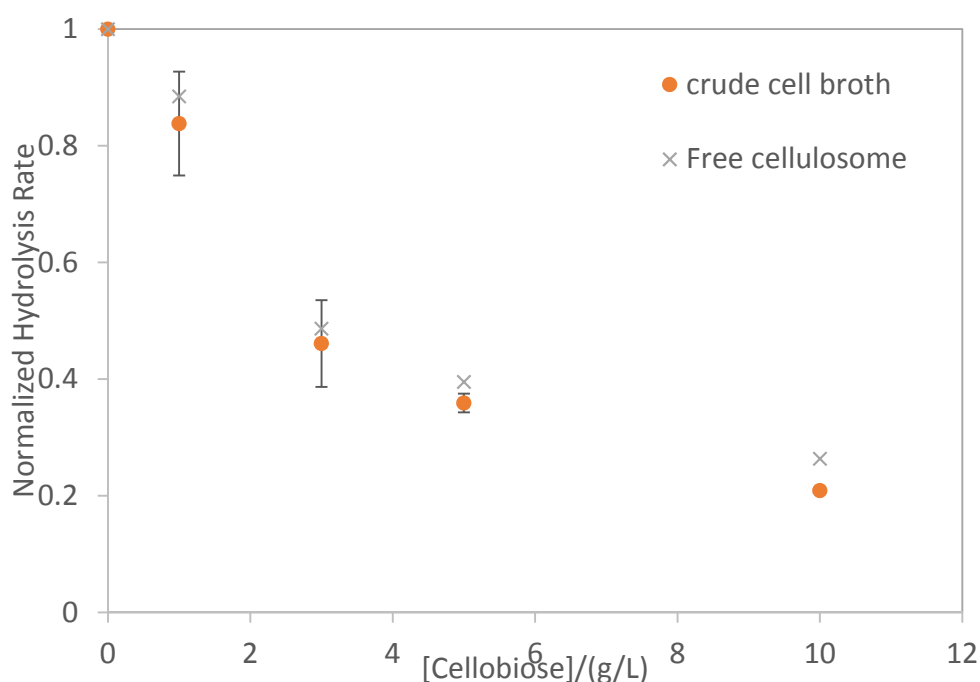
Figure 3.9 Cellobiose inhibition pattern comparison among free cellulosome (no replication) and crude cell broth (error based on three replication).

Conclusion

With the goal of developing techniques to quantify and model the inhibition kinetics of cellulases, the inhibition of crude cell broth and free cellulosome from *C. thermocellum* (stationary phase) by cellobiose was investigated on model amorphous cellulose surfaces using QCM. Crude cell broth and free cellulosomes were shown to have similar inhibition pattern (within a cellobiose concentration less than10g/L), with about 74-79% inhibition at a concentration of 10 g/L. Kinetic models that interpret inhibited initial hydrolysis rate were developed for the flow system, and correlate well the initial hydrolysis rate. However, these models cannot distingusih the inhibition

types (competitive, noncompetitive, uncompetitive inhibition) on the basis of only initial hydrolysis rates. Kinetics models that incorporate celluosome adsorption and cellulose are expected to describe the inhibition mechanism of free cellulosomes and provide insight into hydrolysis event in crude cell broth.

CHAPTER FOUR

Future Work

Current work which demonstrates the ability to analyze the activity of whole-cell cellulases using QCM can be further extended to several areas to study the lignocellulose degradation. The effect of cellulose substrate properties (degree of crystalinity, chemical composition, morphology, pore size distribution and specific surface area) (Rojas et al. 2007) can be further explored by utilizing different cellulose films. For example, thin film of lignocellulosic nanofibrils (LCNFs) which consist of crystalline cellulose I and amorphous region (Ahola et al. 2008a), enables the mimicking of cellulose hydrolysis on more representative substrates of native cellulose. Also, the potential of modeling cellulose hydrolysis by free cellulosome of *C.thermocellum* as measured by QCM offers greats opportunities to study the effect of reaction condition (pH, temperature etc.) and inhibition by end product (cellobiose, ethanol). Moreover, the frequency change of the QCM due to cell adsorption, which cannot be interpreted directly from the conventional mass-loading theory, will need further interpretation for better understanding the interaction between whole cells and cellulose substrate. Progress in these areas will allow for lignocellulosic biofuel production improvement.

As discussed on Chapter 3, the initial hydrolysis rate as a function of inhibitor concentration is not sufficient to determine the inhibition types. To further investigate the inhibition mechanism, fitting the interfacial models of inhibition described by the Michaelis-Menten equations to the entire frequency response, and not just the initial rates, would be required. Here we proposed a kinetic model to illustrate cellulose hydrolysis on sensor surface which is uniformly coated with amorphous cellulose (LiCl/DMAc coated). For example, the scheme of the model for competitive inhibition is:

(i)   The formation of enzyme-inhibitor (EI) is reversible and assumed to be at fast equilibrium since enzyme and inhibitor are mixed well before introducing to QCM cell and reacting with cellulose.

$$E + I \; \underset{k_{-i}}{\overset{k_i}{\longleftrightarrow}} \; EI$$
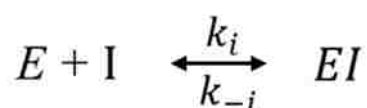
(ii)   The adsorption of enzyme (E) to substrate (S) to form a complex (ES) is reversible and described as n-th order reaction. The formation of inactive enzyme-substrate (ES_i^*) is also assumed to slow down the hydrolysis.

$$E + S_i \underset{k_{-1}}{\overset{k_1}{\rightleftharpoons}} ES_i$$

$$ES_i \xrightarrow{k_3} ES_i^*$$
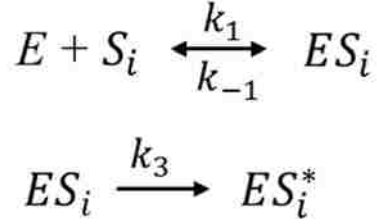
(iii) This complex (ES) then breaks down in a slower step to yield product (P). This model assumes the enzyme progressively hydrolyzes the cellulose. Therefore, enzyme released from enzyme/substrate complex after production formation (i.e. ß-1, 4-glycosidic bond cleavage) will bind to the cellulose chain immediately and slides along the cellulose chain until eventually the cellulose chain dissociates.

$$ES_i \xrightarrow{k_2} ES_i + P$$
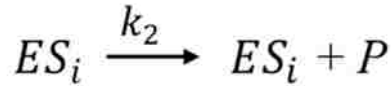
(iv)   The cellulose film is considered as multilayers of cellulose chains. Only the interfacial cellulose sites (S_i) are accessible to cellulase while the bulk cellulose sites (cellulose underlying the interfacial cellulose, S_b) will become interfacial sites as it is exposed to enzyme due to the hydrolysis of interfacial cellulose.

$$S_b \xrightarrow{k_b} S_i$$
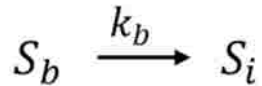
Based on the above kinetic schemes, set of differential equations can be derived to describe cellulase adsorption and hydrolysis.

$$\frac{d[EI]}{dt} = k_i[E][I] - k_{-1}[EI] = 0$$

$$\frac{d[ES_i]}{dt} = k_1[E^n][S_i] - k_{-1}[ES_i] - k_3[ES_i\ ]$$

$$\frac{d[ES_i^*]}{dt} = k_3[ES_i]$$

$$\frac{d[S_i]}{dt} = -k_2[ES_i] + k_b S_b$$

The rate parameters in the model will be obtained by fitting above differential equations to the experimentally measured change in frequency, where the change in

mass of film can be expressed as the sum of mass changes due to enzyme adsorption on the substrate and the mass loss due to hydrolysis ($S_{i,0}$ and $S_{b,0}$ are the initial interfacial and bulk substrate concentration, respectively):

$$\Delta f = -A \left[ES_i + ES_i^*\right] + B\left[(S_{i,0} - S_i) + (S_{b,0} - S_b)\right]$$

$$\text{enzyme adsorption} \qquad \text{hydrolysis}$$

On the basis of proposed kinetic scheme, different inhibition mechanism can be incorporated to examine their ability to describe the QCM frequency profile as a function of inhibitor concentration. According to the fitting condition and reasonability of rate parameters, the final inhibition mechanism can be determined.

The developed kinetic model can also be used to describe the effect of other reaction conditions such as pH or temperature, which affects enzyme activity. The optimum conditions for enzyme hydrolysis and fermentation microorganism growth are usually different. Maximum activity of cellulosome from *C.thermocellum* was reported at 70 ℃ and at pH 5.7 on Avicel (Johnson et al. 1982a). Meanwhile, fermenting yeast and bacteria have optimum growth temperature around 32-37 ℃ (Jorgensen et al. 2007). Consequently, a compromise between optimal temperatures for hydrolysis and fermentation is used, which is less favorable for enzyme hydrolysis. For example, Nakayama et al. (2011) reported that the optimum temperature for butanol production using co-culture of *C.thermocellum* and *Clostridium acetobutylicum* was 30 ℃. Also, the fermentation product of Clostridia such as lactic, acetic acid in addition to solvents will decrease the pH of medium and are inhibitory to cellulase (Li 2012). Therefore, understanding the how the changes of pH and temperature affect the enzyme hydrolysis efficiency will help to design better cellulose fermentation process.

Inhibition by ethanol, the end product of *C.thermocellum* metabolism, should also be addressed. The growth of *C.thermocellum* is strongly inhibited by ethanol at relative low concentrations (5g/L) (Herrero and Gomez 1980) and the cellulase activity of *C.thermocellum* is rather resistant to ethanol, with 50% inhibition at 8 wt% ethanol (Bernardez et al. 1994). Some literature proposed that ethanol caused the changes in the cell membrane and inhibited the glycolytic enzyme activity thus affect the cell growth (Jones 1989, Demain et al. 2005). In the effort to improve and understand ethanol tolerance of *C.thermocellum*, technologies like gradual ethanol-adaption growth (Shao et al. 2011, Rani et al. 1996), genetic engineering (Brown et al. 2011) and chemical or UV mutagenesis is used to obtain to ethanol tolerant stains. In addition to

improving the ethanol tolerance of *C.thermocellum* to reduce ethanol inhibition, another strategy is removing ethanol continuously during the fermentation, which requires the development of ethanol separation process. Also, understanding how ethanol adaptation impacts hydrolytic activity will provide criteria for choosing the separation efficiency and designing the separation process.

APPENDIX A

Initial Rate Expression Development for Inhibited Enzyme Kinetics on Cellulose Thin Film Measured by QCM-D

The hydrolysis activity of cellulases are quantified by initial hydrolysis rate (v_o), which is the maximum slope that covers most of the frequency curve after the minimum frequency. Traditionally, Michaelis-Menten model is used to interpret kinetic data and determine the inhibition types (Holtzapple et al. 1990, Gusakov et al. 1985a). As shown in the following equation, the first step of Michaelis-Menten kinetic is that the enzyme (E) and the substrate (S) combine to form a complex (ES) that is reversible and relatively fast. This complex (ES) then breaks down in a slower step to yield free enzyme (E) and product (P).

$$E + S \underset{k_{-1}}{\overset{k_1}{\rightleftharpoons}} ES \xrightarrow{k_2} E + P$$

However, Michaelis-Menten model is developed under homogenous reaction conditions (Michaelis and Menten 1913). Thus it can't be directly applied to the cellulose hydrolysis happened on amorphous cellulose film, which is a heterogeneous surface reaction. To interpret the cellobiose inhibition mechanism, modified Michaelis-Menten model for continuous flow system (QCM system) was developed for three known inhibition mechanism (competitive, non-competitive, uncompetitive inhibition).

Competitive inhibition

Competitive inhibitor (I) competes with substrate for enzyme active site by forming enzyme-inhibitor complex (EI), which result in reducing hydrolysis activity. Its inhibition scheme can be described as:
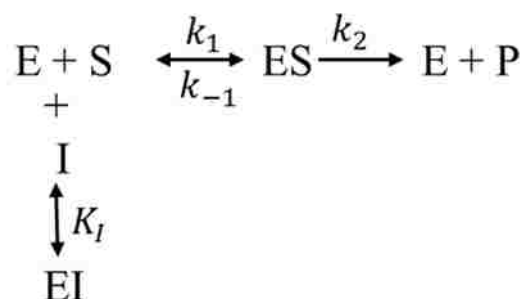
$$E + S \underset{k_{-1}}{\overset{k_1}{\rightleftharpoons}} ES \xrightarrow{k_2} E + P$$
$$+$$
$$I$$
$$\updownarrow K_I$$
$$EI$$

As the cellulose hydrolysis was measured by QCM, enzyme solutions with

inhibitor continuous flowed over cellulose surface. Therefore, the concentration of free enzyme[E], free inhibitor [I] and enzyme-inhibitor complex [EI] was constant during the reaction, which satisfy the following equations:

$$[I] = [I_o] - [EI]$$

$$[E] = [E_o] - [EI]$$

$$[S] = [S_t] - [ES] = [S_0] - [ES] \text{ when time (t)} = 0$$

where $[E_o]$ is the total enzyme concentration, $[I_o]$ is the total inhibitor concentration and $[S_t]$ is the instantaneous substrate concentration equals the total substrate concentration $[S_0]$ at the beginning of reaction.

Assuming ES formation is quasi steady state ($\frac{d[ES]}{dt} = 0$), following differential equation can be derived based on the kinetic scheme:

$$\frac{d[ES]}{dt} = k_1[E][S] - k_{-1}[ES] - k_2[ES] = 0$$

Substitute substrate balance ($[S] = [S_0] - [ES]$) into above equation:

$$\Rightarrow k_1[E]([S_0] - [ES]) - k_{-1}[ES] - k_2[ES] = 0$$

$$\Rightarrow [ES] = \frac{[S_0]}{1 + \frac{k_{-1} + k_2}{k_1[E]}} = \frac{[S_0]}{1 + \frac{K_m}{[E]}}, \qquad K_m = \frac{k_{-1} + k_2}{k_1}$$

Therefore, the initial hydrolysis rate in the presence of inhibitor ($v_{0\_inhibitied}$) can be expressed as:

$$\boldsymbol{v_{0\_inhibitied} = k_2[ES]} = \frac{k_2[S_0]}{1 + \frac{K_m}{[E]}} \quad \textbf{(1)}$$

Assuming the formation of EI is a fast equilibrium ($\frac{d[EI]}{dt} = 0$), following differential equation can be derived based on the kinetic scheme:

$$\frac{d[EI]}{dt} = k_i[E][I] - k_{-i}[EI] = 0$$

which can be transformed into

$$K_I = \frac{k_{-i}}{k_i} = \frac{[E][I]}{[EI]} = \frac{[E][I]}{[E_0] - [E]}$$

$$\Rightarrow \quad \frac{[E_0]}{[E]} = 1 + \frac{[I]}{K_I}$$

$$\Rightarrow \quad [E] = \frac{[E_0]}{1 + \frac{[I]}{K_I}} \quad \textbf{(2)}$$

Similar to the derivation of Eq. (1), for the enzymatic kinetic in the absence of

$$E + S \underset{k_{-1}}{\overset{k_1}{\rightleftharpoons}} ES \overset{k_2}{\longrightarrow} E + P$$

inhibitor (scheme showed above), the initial hydrolysis rate ($v_{0\_uninhibitied}$) can be derived as:

$$v_{0\_uninhibitied} = k_2[ES] = \frac{k_2[S_0]}{1 + \frac{K_m}{[E]}}$$

Specially, without the presence of inhibitor, the free enzyme concentration [E] equals total enzyme concentration $[E_0]$, which is constant during the reaction. Therefore, the initial hydrolysis rate in the presence of inhibitor ($v_{0\_inhibitied}$) can be expressed as:

$$\boldsymbol{v_{0\_uninhibitied} = k_2[ES] = \frac{k_2[S_0]}{1 + \frac{K_m}{[E_0]}}} \quad (3)$$

To derivate the relation between $v_{0\_inhibitied}$ and $v_{0\_uninhibitied}$, Eq. (1) and (3) are transformed as shown below:

$$v_{0\_inhibitied} = \frac{k_2[S_0]}{1 + \frac{K_m}{[E]}} \qquad \Rightarrow \qquad \frac{1}{v_{0\_inhibitied}} = \frac{1}{k_2[S_0]} + \frac{K_m}{k_2[S_0][E]}$$

$$v_{0\_uninhibitied} = \frac{k_2[S_0]}{1 + \frac{K_m}{[E_0]}} \qquad \Rightarrow \qquad \frac{1}{v_{0\_uninhibitied}} = \frac{1}{k_2[S_0]} + \frac{K_m}{k_2[S_0][E_0]}$$

Therefore:

$$\frac{1}{v_{0\_inhibitied}} - \frac{1}{v_{0uninhibitied}} = \frac{K_m}{k_2[S_0]}\left(\frac{1}{[E]} - \frac{1}{[E_0]}\right)$$

Substitute Eq. (2) into above equation, obtained

$$\frac{1}{v_{0inhibitied}} - \frac{1}{v_{0uninhibitied}} = \frac{K_m}{k_2[S_0]}\left(\frac{1}{[E]} - \frac{1}{[E_0]}\right) = \frac{K_m}{k_2[S_0]}\left(\frac{1 + \frac{[I]}{K_I}}{[E_0]} - \frac{1}{[E_0]}\right)$$

Therefore, the inhibited initial rate expression as a function of inhibitor concentration is obtained:

$$\boldsymbol{\frac{1}{v_{0inhibitied}} - \frac{1}{v_{0uninhibitied}} = \frac{K_m}{k_2K_I\,[S_0][E_0]}[I]} \quad (4)$$

Noncompetitive inhibition

Noncompetitive inhibitor (I) can bind to the allosteric sites other than the active sites of either enzyme or enzyme-substrate complex, which prevents the product formation and reducing hydrolysis activity. Its inhibition scheme can be described as:

$$E + S \xrightleftharpoons[k_{-1}]{k_1} ES \xrightarrow{k_2} E + P$$

$$EI + S \xrightleftharpoons[k_{-1}]{k_1} ESI$$

As the cellulose hydrolysis was measured by QCM, enzyme solutions with inhibitor continuously flowed over cellulose surface. Therefore, the concentration of free enzyme $[E]$, free inhibitor $[I]$ and enzyme-inhibitor complex $[EI]$ was constant during the reaction, which satisfy the following equations:

$[I] = [I_o] - [EI]$

$[E] = [E_o] - [EI]$

$[S] = [S_t] - [ES] - [ESI] = [S_0] - [ES] - [ESI]$ when time (t) =0

where $[E_o]$ is the total enzyme concentration, $[I_o]$ is the total inhibitor concentration and $[S_t]$ is the instantaneous substrate concentration equals the total substrate concentration $[S_0]$ at the beginning of reaction.

Assuming ES formation is quasi steady state ($\frac{d[ES]}{dt} = 0$) and the formation of ESI is a fast equilibrium ($\frac{d[ESI]}{dt} = 0$), following differential equation can be derived based on the kinetic scheme:

$$\frac{d[ESI]}{dt} = k_i[ES][I] - k_{-i}[ESI] = 0$$

$$\Rightarrow K_I = \frac{k_{-i}}{k_i} = \frac{[ES][I]}{[ESI]} \Rightarrow [ESI] = \frac{[I]}{K_I}[ES]$$

$$\frac{d[ES]}{dt} = k_1[E][S] - k_{-1}[ES] - k_2[ES] + (k_{-i}[ESI] - k_i[ES][I]) = 0$$

$$\Rightarrow \frac{d[ES]}{dt} = k_1[E][S] - k_{-1}[ES] - k_2[ES] = 0$$

Substitute substrate balance($[S] = [S_0] - [ES] - [ESI]$) into above equation:

$$\Rightarrow k_1[E]([S_0] - [ES] - [ESI]) - k_{-1}[ES] - k_2[ES] = 0$$

$$\Rightarrow k_1[E]([S_0] - [ES] - \frac{[I]}{K_I}[ES]) - k_{-1}[ES] - k_2[ES] = 0$$

$$\Rightarrow [ES] = \frac{[S_0]}{1 + \frac{[I]}{K_I} + \frac{k_{-1} + k_2}{k_1[E]}} = \frac{[S_0]}{1 + \frac{[I]}{K_I} + \frac{K_m}{[E]}}, \quad K_m = \frac{k_{-1} + k_2}{k_1}$$

Therefore, the initial hydrolysis rate in the presence of inhibitor ($v_{0\_inhibitied}$) can be expressed as:

$$v_{0\_inhibitied} = k_2[ES] = \frac{k_2[S_0]}{1 + \frac{[I]}{K_I} + \frac{K_m}{[E]}} \quad (5)$$

Assuming the formation of EI is a fast equilibrium ($\frac{d[EI]}{dt} = 0$), following differential equation can be derived based on the kinetic scheme:

$$\frac{d[EI]}{dt} = k_i[E][I] - k_{-i}[EI] = 0$$

which can be transformed into

$$K_I = \frac{k_{-i}}{k_i} = \frac{[E][I]}{[EI]} = \frac{[E][I]}{[E_0] - [E]}$$

$$\Rightarrow \frac{[E_0]}{[E]} = 1 + \frac{[I]}{K_I}$$

$$\Rightarrow [E] = \frac{[E_0]}{1 + \frac{[I]}{K_I}} \quad (6)$$

To derivate the relation between $v_{0\_inhibitied}$ and $v_{0\_uninhibitied}$, Eq. (5) and (3) are transformed as shown below:

$$v_{0\_inhibitied} = \frac{k_2[S_0]}{1 + \frac{[I]}{K_I} + \frac{K_m}{[E]}} \Rightarrow \frac{1}{v_{0\_inhibitied}} = \frac{1}{k_2[S_0]} + \frac{[I]}{k_2 K_I[S_0]} + \frac{K_m}{k_2[S_0][E]}$$

$$v_{0\_uninhibitied} = \frac{k_2[S_0]}{1 + \frac{K_m}{[E_0]}} \Rightarrow \frac{1}{v_{0\_uninhibitied}} = \frac{1}{k_2[S_0]} + \frac{K_m}{k_2[S_0][E_0]}$$

Therefore,

$$\frac{1}{v_{0\_inhibitied}} - \frac{1}{v_{0uninhibitied}} = \frac{[I]}{k_2 K_I[S_0]} + \frac{K_m}{k_2[S_0]}\left(\frac{1}{[E]} - \frac{1}{[E_0]}\right)$$

$$= \frac{[I]}{k_2 K_I[S_0]} + \frac{K_m}{k_2 K_I \ [S_0][E_0]}[I] = \frac{1}{k_2 K_I[S_0]}(1 + \frac{K_m}{[E_0]})[I]$$

Substitute Eq. (6) into above equation, obtained

$$\frac{1}{v_{0_{inhibitied}}} - \frac{1}{v_{0_{uninhibitied}}} == \frac{[I]}{k_2 K_I [S_0]} + \frac{K_m}{k_2 [S_0]} \left(\frac{1 + \frac{[I]}{K_I}}{[E_0]} - \frac{1}{[E_0]} \right)$$
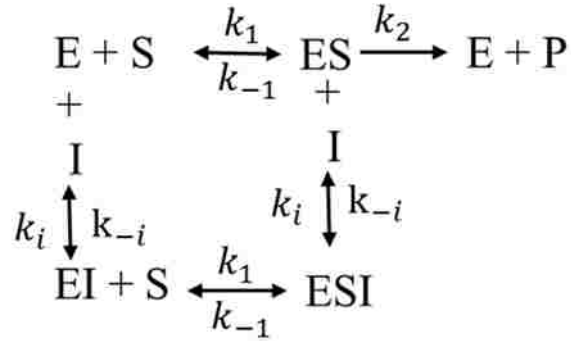
Therefore, the inhibited initial rate expression as a function of inhibitor concentration is obtained:

$$\frac{1}{v_{0_{inhibitied}}} - \frac{1}{v_{0_{uninhibitied}}} = \frac{1}{k_2 K_I [S_0]} \left(1 + \frac{K_m}{[E_0]} \right) [I] \quad (7)$$

Uncompetitive inhibition

Uncompetitive inhibitor (I) can bind only binds to the enzyme-substrate complex to reduce enzyme-substrate complex concentration and lead to reduced hydrolysis activity. Its inhibition scheme can be described as:

$$E + S \underset{k_{-1}}{\overset{k_1}{\rightleftharpoons}} ES \overset{k_2}{\longrightarrow} E + P$$
$$+$$
$$I$$
$$k_i \updownarrow k_{-i}$$
$$ESI$$

As the cellulose hydrolysis was measured by QCM, enzyme solutions with inhibitor continuously flowed over cellulose surface. Therefore, the concentration of free enzyme[E], free inhibitor [I] was constant during the reaction, which satisfy the following equations:

[I] = $[I_o]$

[E] = $[E_o]$

$[S] = [S_t] - [ES] - [ESI] = [S_0] - [ES] - [ESI]$ when time (t) =0

where $[E_o]$ is the total enzyme concentration, $[I_o]$ is the total inhibitor concentration and $[S_t]$ is the instantaneous substrate concentration equals the total substrate concentration$[S_0]$ at the beginning of reaction.

Assuming ES formation is quasi steady state ($\frac{d[ES]}{dt} = 0$) and the formation of ESI is a fast equilibrium ($\frac{d[ESI]}{dt} = 0$), following differential equation can be derived based on the kinetic scheme:

$$\frac{d[ESI]}{dt} = k_i[ES][I] - k_{-i}[ESI] = 0$$

$$\Rightarrow K_I = \frac{k_{-i}}{k_i} = \frac{[ES][I]}{[ESI]} \Rightarrow [ESI] = \frac{[I]}{K_I}[ES]$$

$$\frac{d[ES]}{dt} = k_1[E][S] - k_{-1}[ES] - k_2[ES] + (k_{-i}[ESI] - k_i[ES][I]) = 0$$

$$\Rightarrow \frac{d[ES]}{dt} = k_1[E][S] - k_{-1}[ES] - k_2[ES] = 0$$

Substitute substrate balance($[S] = [S_0] - [ES] - [ESI]$) into above equation:

$$\Rightarrow k_1[E]([S_0] - [ES] - [ESI]) - k_{-1}[ES] - k_2[ES] = 0$$

$$\Rightarrow k_1[E]([S_0] - [ES] - \frac{[I]}{K_I}[ES]) - k_{-1}[ES] - k_2[ES] = 0$$

$$\Rightarrow [ES] = \frac{[S_0]}{1 + \frac{[I]}{K_I} + \frac{k_{-1} + k_2}{k_1[E]}} = \frac{[S_0]}{1 + \frac{[I]}{K_I} + \frac{K_m}{[E]}}, \qquad K_m = \frac{k_{-1} + k_2}{k_1}$$

Therefore, the initial hydrolysis rate in the presence of inhibitor ($v_{0\_inhibitied}$) can be expressed as:

$$v_{0\_inhibitied} = k_2[ES] = \frac{k_2[S_0]}{1 + \frac{[I]}{K_I} + \frac{K_m}{[E]}}$$

Since $[E] = [E_o]$, $[I] = [I_o]$, so

$$\boldsymbol{v_{0\_inhibitied} = k_2[ES] = \frac{k_2[S_0]}{1 + \frac{[I_0]}{K_I} + \frac{K_m}{[E_0]}}} \qquad (\mathbf{8})$$

To derivate the relation between $v_{0\_inhibitied}$ and $v_{0\_uninhibitied}$, Eq. (8) and (3) are transformed as shown below:

$$v_{0\_inhibitied} = \frac{k_2[S_0]}{1 + \frac{[I_0]}{K_I} + \frac{K_m}{[E_0]}} \Rightarrow \frac{1}{v_{0\_inhibitied}} = \frac{1}{k_2[S_0]} + \frac{[I_0]}{k_2 K_I[S_0]} + \frac{K_m}{k_2[S_0][E_0]}$$

$$v_{0\_uninhibitied} = \frac{k_2[S_0]}{1 + \frac{K_m}{[E_0]}} \Rightarrow \frac{1}{v_{0\_uninhibitied}} = \frac{1}{k_2[S_0]} + \frac{K_m}{k_2[S_0][E_0]}$$

Therefore,

$$\frac{1}{v_{0\_inhibitied}} - \frac{1}{v_{0_{uninhibitied}}} = \frac{[I_0]}{k_2 K_I[S_0]}$$

Therefore, the inhibited initial rate expression as a function of inhibitor concentration is obtained:

$$\frac{1}{v_{0_{inhibitied}}} - \frac{1}{v_{0_{uninhibitied}}} = \frac{[I_0]}{k_2 K_I [S_0]} \quad (9)$$

In summary, the inhibited initial rate expression as a function of inhibitor concentration for competitive, noncompetitive and uncompetitive inhibition are Eq. (4), (7), (9) respectively. As shown below, $\frac{1}{v_{0_{inhibitied}}} - \frac{1}{v_{0_{uninhibitied}}}$ are all linear to inhibitor concentration, which makes it unable to decide the inhibition types. Furthermore, Fig.A.1 shows a linear relationship between $\frac{1}{v_{0_{inhibitied}}} - \frac{1}{v_{0_{uninhibitied}}}$ and cellobiose concentration which is based on the inhibition experiment of the crude cell broth of *C.thermocellum* measured by QCM on amorphous cellulose film at 50 ºC.

$$\frac{1}{v_{0_{inhibitied}}} - \frac{1}{v_{0_{uninhibitied}}} = \frac{K_m}{k_2 K_I [S_0][E_0]}[I] \quad (4)$$

$$\frac{1}{v_{0_{inhibitied}}} - \frac{1}{v_{0_{uninhibitied}}} = \frac{1}{k_2 K_I [S_0]}\left(1 + \frac{K_m}{[E_0]}\right)[I] \quad (7)$$

$$\frac{1}{v_{0_{inhibitied}}} - \frac{1}{v_{0_{uninhibitied}}} = \frac{[I]}{k_2 K_I [S_0]} \quad (9)$$
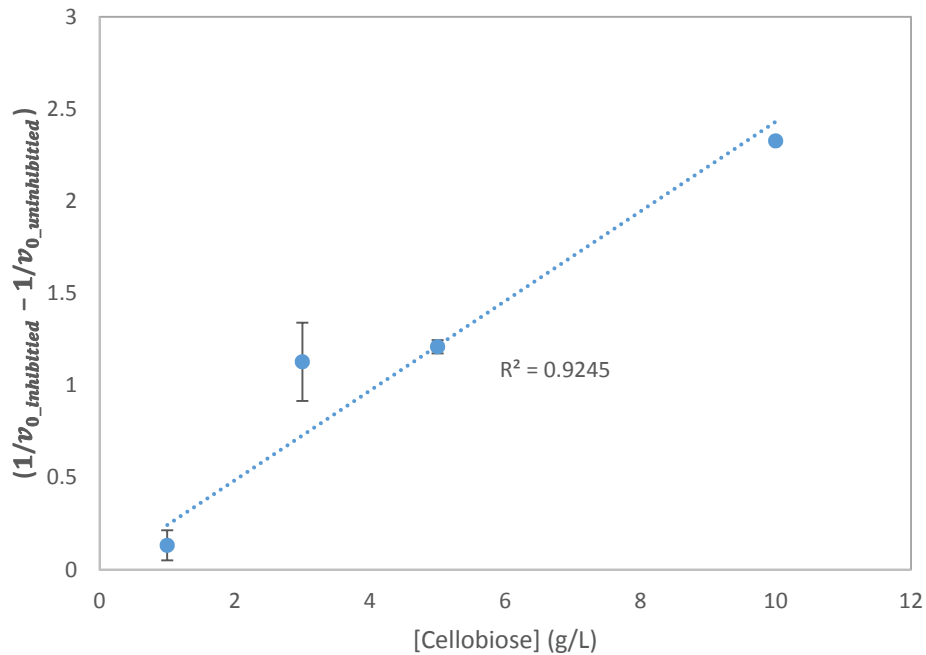
Figure A.1 Cellobiose inhibited initial hydrolysis rate of crude cell broth of *C.thermocellum* as a function of cellobiose concentration measured by QCM on amorphous cellulose film at 50 ºC.

REFERENCE

Ahola, S., J. Salmi, L.-S. Johansson, J. Laine, and M. Österberg. 2008a. "Model Films from Native Cellulose Nanofibrils. Preparation, Swelling, and Surface Interactions." *Biomacromolecules* no. 9:1273–1282.

Ahola, S., X. Turon, M. Osterberg, J. Laine, and O. J. Rojas. 2008b. "Enzymatic Hydrolysis of Native Cellulose Nanofibrils and Other Cellulose Model Films: Effect of Surface Structure." *Langmuir* no. 24:11592-11599.

Aulin, C., S. Ahola, P. Josefsson, T. Nishino, Y. Hirose, M. Osterberg, and L. Wagberg. 2009. "Nanoscale cellulose films with different crystallinities and mesostructures--their surface properties and interaction with water." *Langmuir* no. 25 (13):7675-85.

Bansal, P., M. Hall, M. J. Realff, J. H. Lee, and A. S. Bommarius. 2009. "Modeling cellulase kinetics on lignocellulosic substrates." *Biotechnol Adv* no. 27 (6):833-48.

Bayer, E A, R Kenig, and R Lamed. 1983. "Adherence of Clostridium thermocellum to Cellulose." *J. Bacteriol.* no. 156 (2):818-827.

Bayer, E A, and R Lamed. 1986. "Ultrastructure of the cell surface cellulosome of Clostridium thermocellum and its interaction with cellulose." *J Bacteriol.* no. 167 (3):828-836.

Bayer, E A, E Setter, and R Lamed. 1985. "Organization and Distribution of the Cellulosome in Clostridium thermocellum." *J. Bacteriol.* no. 163 (2):552-559.

Bayer, E. A., J. P. Belaich, Y. Shoham, and R. Lamed. 2004. "The cellulosomes: multienzyme machines for degradation of plant cell wall polysaccharides." *Annu Rev Microbiol* no. 58:521-54.

Bayer, Edward A., Ely Morag, and Raphael Lamed. 1994. "The cellulosome - a treasuretrove for biotechnology." *Trends Biotechnol.* no. 12 (9):379-386.

Bayer, Edward A., Linda J. W. Shimon, Yuval Shoham, and Raphael Lamed. 1998. "Cellulosomes—Structure and Ultrastructure." *Journal of structural biology* no. 124:221-234.

Bernardez, T. D., K. A. Lyford, and L. R. Lynd. 1994. "Kinetics of the extracellular cellulases of *Clostridium thermocellum* acting on pretreated mixed hardwood and Avicel." *Applied Microbiology and Biotechnology* no. 41 (5):620-625.

Bolam, D N, A Ciruela, S McQueen-Mason, P Simpson, M P Williamson, A Boraston J E Rixon, G P Hazlewood, and H J Gilbert. 1998. "Pseudomonas cellulose-binding domains mediate their effects by increasing enzyme substrate proximity." *Biochem J.* no. 331 (Pt 3):775-781.

Boraston, Alisdair B., David N. Bolam, Harry J. Gilbert, and Gideon J. Davies. 2004. "Carbohydrate-binding modules fine-tuning polysaccharide recognition." *Biochem. J.* no. 382:769-781.

Bothun, Geoffrey D. 2004. *PRESSURIZED SOLVENTS IN WHOLE-CELL BIOPROCESSING: METABOLIC AND STRUCTURAL PERTURBATIONS*, Department of Chemical Engineering, University of Kentucky, Lexington, Kentucky.

Brown, Steven D., Adam M. Gussa, Tatiana V. Karpinetsa, Jerry M. Parksa, Nikolai Smolin, Shihui Yang, Miriam L. Land, Dawn M. Klingeman, Ashwini Bhandiwad, Miguel Rodriguez, Jr. Babu Raman, Xiongjun Shao, Jonathan R. Mielenz, Eremy C. Smith, Martin Keller, and Lee R. Lynd. 2011. "Mutant alcohol dehydrogenase leads to improved ethanol tolerance in *Clostridium thermocellum*." *Proc Natl Acad Sci USA* no. 108:13752-13757.

Campbell, Malcolm M., and Ronald R. Sederoff. 1996. "Variation in Lignin Content and Composition." *Plant Physiol.* no. 110:3-13.

Carrard, G., Koivula, A., Soderlund, H. and Beguin, P. . 2000. "Cellulose-binding domains promote hydrolysis of different sites on crystalline cellulose." *Proc.*

Natl. Acad. Sci. U.S.A. no. 97:10342–10347.

Chang, Vincent S., and Mark T. Holtzapple. 2000. "Fundamental factors affecting biomass enzymatic reactivity." *Appl Biochem Biotech* no. 84-86:5-37.

Chang, Vincent S., Murlidhar Nagwani, Chul-Ho Kim, and Mark T. Holtzapple. 2001. "Oxidative lime pretreatment of high-lignin biomass." *Applied Biochemistry and Biotechnology* no. 94 (1):1-28.

Choi, S. K., and L. G. Ljungdahl. 1996. "Structural role of calcium for the organization of the cellulosome of *Clostridium thermocellum*." *Biochemistry* no. 35:4906–4910.

Demain, A. L., M. Newcomb, and J. H. Wu. 2005. "Cellulase, clostridia, and ethanol." *Microbiol Mol Biol Rev* no. 69 (1):124-54.

Din, N., H. G. Damude, N. R. Gilkes, R. C. J. Miller, R. A. J. Warren, and D. G. Kilburn. 1994. "C1-Cx revisited: Intramolecular synergism in a cellulase." *Proc. Natl. Acad. Sci. USA* no. 91:1183-11387.

Din, N., N. R. Gilkes, B. Tekant, R. C. J. Miller, R. A. J. Warren, and D. G. Kilburn. 1991. "Non-hydrolytic disruption of cellulose fibres by the binding domain of a bacterial cellulase." *Biotechnology* no. 9:1096–1099.

Ding, S. Y., Y. S. Liu, Y. Zeng, M. E. Himmel, J. O. Baker, and E. A. Bayer. 2012. "How does plant cell wall nanoscale architecture correlate with enzymatic digestibility?" *Science* no. 338 (6110):1055-60.

Dixon, Matthew C. 2008. "Quartz Crystal Microbalance with Dissipation Monitoring Enabling Real-Time Characterization of Biological Materials and Their Interactions." no. 19:151-158.

Drissen, R.E.T., R.H.W. Maas, M.J.E.C. van der Maarel, M.A. Kabel, H.A. Schols, J. Tramper, and H.H. Beeftink. 2007. "A generic model for glucose production fromvarious cellulose sources by a commercial cellulase complex." *Biocatal*

Biotransfor no. 25:419-429.

Dumitrache, A., G. Wolfaardt, G. Allen, S. N. Liss, and L. R. Lynd. 2013. "Form and function of Clostridium thermocellum biofilms." *Appl Environ Microbiol* no. 79 (1):231-9.

Dupont, C. 2003. *Gelatine sizing of paper and its impact on the degradation of cellulose during aging: a study using size-exclusion chromotography*, Van 't Hoff Institute for Molecular Sciences, University of Van Amsterdam, Amsterdam.

Eriksson, J., M. Malmsten, F. Tiberg, T. H. Callisen, T. Damhus, and K. S. Johansen. 2005. "Enzymatic degradation of model cellulose films." *J Colloid Interface Sci* no. 284 (1):99-106.

Ferreira, G. N., A. C. Silva, and B. Tome. 2009. "Acoustic wave biosensors: physical models and biological applications of quartz crystal microbalance." *Trends Biotechnol* no. 27 (12):689-97.

Freier, Doris, Cheryle P. Mothershed, and Juergen Wiegel. 1988. "Characterization of Clostridium thermocellum JW20." *Appl. Environ. Microbiol.* no. 54 (1):204-211.

Fujino, T., P. Be´guin, and J. P. Aubert. 1993. "Organization of a Clostridium thermocellum gene cluster encoding the cellulosomal scaffolding protein CipA and a protein possibly involved in attachment of the cellulosome to the cell surface." *J. Bacteriol.* no. 175:1891-1899.

Gao, P. J., Chen, G. J., Wang, T. H., Zhang, Y. S. and Liu, J. 2001. "Non-hydrolytic disruption of crystalline structure of cellulose by cellulose binding domain and linker sequence of cellobiohydrolase I from *Penicillium janthinellum*." *Shengwu Huaxue Yu Shengwu Wuli Xuebao* no. 33:13-18.

Gerngross, U. T., M. P. M. Romainiec, N. S. Huskisson, and A. L. Demain. 1993. "Sequencing of a *Clostridium thermocellum* gene (cipA) encoding the cellulosomal SL-protein reveals an unusual degree of internal homology." *Mol. Microbiol.* no. 8:325-334.

Gruno, M., P. Valjamae, G. Pettersson, and G. Johansson. 2004. "Inhibition of the Trichoderma reesei cellulases by cellobiose is strongly dependent on the nature of the substrate." *Biotechnol Bioeng* no. 86 (5):503-11.

Gusakov, A.V., A.P. Sinitsyn, V.B. Gerasimas, R.Yu. Savitskene, and Yu.Yu. Steponavichus. 1985a. "A product inhibition study of cellulases from *Trichoderma longibrachiatum* using dyed cellulose." *J Biotechnol* no. 3:167–174.

Gusakov, A.V., A.P. Sinitsyn, and A.A. Klyosov. 1985b. "Kinetics of the enzymatic hydrolysis of cellulose: 1. A mathematical model for a batch reactor process." *Enzyme Microb Technol* no. 7:346-352.

Hasunuma, Tomohisa, and Akihiko Kondo. 2012. "Consolidated bioprocessing and simultaneous saccharification and fermentation of lignocellulose to ethanol with thermotolerant yeast strains." *Process Biochemistry* no. 47 (9):1287-1294.

Herrero, Alejandro A., and Reinaldo F. Gomez. 1980. "Development of Ethanol Tolerance in *Clostridium thermocellum*: Effect of Growth Temperature." *Appl Environ Microbiol.* no. 40 (3):571-577.

Himmel, M. E., S. Y. Ding, D. K. Johnson, W. S. Adney, M. R. Nimlos, J. W. Brady, and T. D. Foust. 2007. "Biomass Recalcitrance: Engineering Plants and Enzymes for Biofuels Production." *Science* no. 315 (5813):804-807.

Holmberg, M., J. Berg, S. Stemme, L. Oedberg, J. Rasmusson, and P. J. Claesson. 1997. "Surface Force Studies of Langmuir–Blodgett Cellulose Films." *J. Colloid Interface Sci.* no. 186:369-381.

Holtzapple, M, M Cognata, Y Shu, and C Hendrickson. 1990. "Inhibition of *Trichoderma reesei* Cellulase by Sugars and Solvents." *Biotechnol Bioeng* no. 36:275-287.

Hu, Gang. 2009. *Adsorption and Activity of Cellulase Enzymes on Various Cellulose Substrates*, Department of Forest Biomaterials, North Carolina State University,

Raleigh, North Carolina.

Hu, Gang, John A. Heitmann, and Orlando J. Rojas. 2009. "In Situ Monitoring of Cellulase Activity by Microgravimetry with a Quartz Crystal Microbalance." *J. Phys. Chem. B* no. 113 (44):14761-14768.

Itoh, Atsushi, and Motoko Ichihashi. 2008. "A frequency of the quartz crystal microbalance (QCM) that is not affected by the viscosity of a liquid." *Measurement Science and Technology* no. 19 (7):075205.

Johnson, Eric A., Frederique Bouchots, and Arnold L. Demain. 1989. "Regulation of cellulase Formation in Clostvidium thermocellum." *Journal of General Microbiology* no. 131:2303-2308.

Johnson, Eric A., Mitsuji Sakajoh, Geoffrey Halliwell, Ashwin Madia, and Arnold L. Demain. 1982a. "Saccharification of complex cellulosic substrates by the cellulase system from *clostridium thermocellum.*" *Appl Environ Microbiol.* no. 43 (5):1125-1132.

Johnson, Eric, Elwyn Reese, and Arnold L.Demain. 1982b. "Inhibition of C. thermocellum cellulase by end products of cellulolysis." *J Appl Biochem* no. 4:64-71.

Jones, Rodney P. 1989. "Biological principles for the effects of ethanol." *Enzyme and Microbial Technology* no. 11 (3):130-153.

Jorgensen, Henning, Jan Bach Kristensen, and Claus Felby. 2007. "Enzymatic conversion of lignocellulose into fermentable sugars: challenges and opportunities." *Biofuels, Bioproducts and Biorefining* no. 1 (2):119-134.

Kim, Sehoon, and Mark T. Holtzapple. 2006. "Effect of structural features on enzyme digestibility of corn stover." *Bioresource Technol* no. 97:583-591.

Kopelman, Raoul. 1988. "Fractal Reaction Kinetics." *Science* no. 241 (4873):1620-1626.

Kruus, K., A. Andreacchi, W. K. Wang, and J. H. David Wu. 1995. "Product inhibition of the recombinant CelS, an exoglucanase component of the Clostridium thermocellum cellulosome." *Appl Microbiol Biotechnol* no. 44:399-404.

Kumagai, A., S. H. Lee, and T. Endo. 2013. "Thin film of lignocellulosic nanofibrils with different chemical composition for QCM-D study." *Biomacromolecules* no. 14 (7):2420-6.

Kumar, Parveen, Diane M. Barrett, Michael J. Delwiche, and Pieter Stroeve. 2009. "Methods for Pretreatment of Lignocellulosic Biomass for Efficient Hydrolysis and Biofuel Production." *Industrial & Engineering Chemistry Research* no. 48 (8):3713-3729.

Lamed, R, E Setter, and E A Bayer. 1983. "Characterization of a cellulose-binding cellulase-containing complex in *clostridium thermocellum*." *J Bacteriol.* no. 156 (2):828-836.

Lamed, Raphael, Rina Kenig, and Eva Setter. 1985. "Major characteristics of the cellulolytic system of Clostridium thermocellum coincide with those of the purified cellulosome." *Enzyme Microb. Technol.* no. 7:35-41.

Li, Hsin-Fen. 2012. *APPLICATION OF THIN FILM ANALYSIS TECHNIQUES AND CONTROLLED REACTION ENVIRONMENTS TO MODEL AND ENHANCE BIOMASS UTILIZATION BY CELLULOLYTIC BACTERIA*, Chemical and Materials Engineering, University of Kentucky, Lexington, KY.

Lineweaver, H , and D. Burk. 1934. "The Determination of Enzyme Dissociation Constants." *Journal of the American Chemical Society* no. 56 (3):658-666.

Lu, Yanpin, Yi-Heng Percival Zhang, and Lee R. Lynd. 2006. "Enzyme-microbe synergy duing cellulose hydrolysis by clostridium thermocellum." *PNAS* no. 103 (44):16165-16169.

Lynd, L. R., W. H. van Zyl, J. E. McBride, and M. Laser. 2005. "Consolidated bioprocessing of cellulosic biomass: an update." *Curr Opin Biotechnol* no. 16

(5):577-83.

Lynd, L. R., P. J. Weimer, W. H. Van Zyl, and I. S. Pretorius. 2002. "Microbial Cellulose Utilization: Fundamentals and Biotechnology." *Microbiology and Molecular Biology Reviews* no. 66 (3):506-577.

Maki, Miranda, Kam Tin Leung, and Wensheng Qin. 2009. "The prospects of cellulase-producing bacteria for the bioconversion of lignocellulosic biomass." *Int. J. Biol. Sci.* no. 5 (5):500-516.

Marju Gruno, Priit Väljamäe, Göran Pettersson andGunnar Johansson. 2004. "Inhibition of the Trichoderma reesei cellulases by cellobiose is strongly dependent on the nature of the substrate." *Biotechnology and Bioengineering* no. 86 (5):503-511.

Martin, S. J., K. O. Wessendog, C. T. Gebert., G. C. Frye, R. W. Cernosek, L. Casaus, and M. A. Mitchell. 1993. "Measuring liquid properties with smooth- and textured-surface resonators." *Proc. IEEE Int. Freq. Control Symp.* no. 47:603-608.

Maurer, S.A., N.W. Brady, N.P. Fajardo, and C.J. Radke. 2013. "Surface kinetics for cooperative fungal cellulase digestion of cellulose from quartz crystal microgravimetry." *Journal of Colloid and Interface Science* no. 394:498-508.

Maurer, Samuel A., Claire N. Bedbrook, and Clayton J. Radke. 2012. "Competitive Sorption Kinetics of Inhibited Endo- and Exoglucanases on a Model Cellulose Substrate." *Langmuir* no. 28:14598-14608.

Maurer, Samuel Andrew. 2012. *Surface-Based Assays for Enzyme Adsorption and Activity on Model Cellulose Films*, Chemical Engineering, University of California, California.

Mayer, Frank, Michael P. Goughlan, YUTAKA MORI, and LARS G. LJUNGDAHL. 1987. "Macromolecular Organization of the Cellulolytic Enzyme Complex of Clostridium thermocellum as Revealed by Electron Microscopy." *Appl. Environ.*

Microbiol. no. 53 (12):2785-2792.

McCleary, B. V. . 1991. "Measurement of Polysaccharide Degrading Enzymes using Chromogenic and Colorimetric Substrates." *Chemistry in Australia* no. 9:398-401.

McCleary, Barry V., and Ida Shameer. 1987. "ASSAY OF MALT β-GLUCANASE USING AZO-BARLEY GLUCAN: AN IMPROVED PRECIPITANT." *Journal of the Institute of Brewing* no. 93 (2):87-90.

McCormick, Charles L., Peter A. Callais, and Brewer H. Hutchinson Jr. 1985. "Solution studies of cellulose in lithium chloride and N,N-dimethylacetamide." *Macromolecules* no. 18 (12):2394-2401.

Michaelis, L., and ML. Menten. 1913. "Die Kinetik der Invertinwirkung." *Biochem Z* no. 49:333-369.

Morag, E., E. A. Bayer, and R. Lamed. 1992. "Unorthodox intra-subunit interactions in the cellulosome of *Clostridium thermocellum*." *Appl. Biochem. Biotechnol.* no. 33:205-217.

Morgenstern, B. , and HW. Kammer. 1996. "Solvation in cellulose LiCl-DMAc solutions." *Trends Polym. Sci.* no. 4 (3):87-92.

Nakayama, S., K. Kiyoshi, T. Kadokura, and A. Nakazato. 2011. "Butanol production from crystalline cellulose by cocultured *Clostridium thermocellum* and Clostridium saccharoperbutylacetonicum N1-4." *Appl Environ Microbiol* no. 77 (18):6470-5.

Ng, T. K., P. J. Weimer, and J. G. Zeikus. 1977. "Cellulolytic and physiological properties of *Clostridium thermocellum*." *Archives of Microbiology* no. 114 (1):1-7.

Notley, Shannon M., Malin Eriksson, Lars Wågberg, Stephanie Beck, and Derek G. Gray. 2006. "Surface Forces Measurements of Spin-Coated Cellulose Thin

Films with Different Crystallinity." *Langmuir* no. 22:3154-3160.

Ohmine, K, H Ooshima, and Y Harano. 1983. "Kinetic study on enzymatic hydrolysis of cellulose by cellulase from *Trichoderma Viride*." *Biotechnol Bioeng* no. 25:2041-2053.

Olsson, A. L., H. C. van der Mei, H. J. Busscher, and P. K. Sharma. 2011. "Acoustic sensing of the bacterium-substratum interface using QCM-D and the influence of extracellular polymeric substances." *J Colloid Interface Sci* no. 357 (1):135-8.

Olsson, Adam L. J., Henny C. Van der Mei, Henk J. Busscher, and Prashant K. Sharma. 2009. "Influence of Cell Surface Appendages on the Bacterium-Substratum Interface Measured Real-Time Using QCM-D." *Langmuir* no. 25:1627-1632.

Olsson, Adam L. J., Henny C. van der Mei, Henk J. Busscher, and Prashant K. Sharma. 2010. "Novel analysis of bacterium-substratum bond maturation measured using a quartz crystal microbalance." *Langmuir* no. 26 (13):11113-7.

Pardo, A. G., and F. Forchiassin. 1999. "Influence of temperature and pH on cellulase activity and stability in Nectria catalinensis." *Revista Argentina de Microbiologia* no. 31 (1):31-35.

Raman, Babu, Chongle Pan, Gregory B. Hurst, Miguel Rodriguez, Catherine K. McKeown, Patricia K. Lankford, Nagiza F. Samatova, and Jonathan R. Mielenz. 2009. "Impact of Pretreated Switchgrass and Biomass Carbohydrates on Clostridium thermocellum ATCC 27405 Cellulosome Composition: A Quantitative Proteomic Analysis." *PLoS ONE* no. 4 (4):e5271.

Rani, K. S., M. V. Swamy, D. Sunitha, D. Haritha, and G. Seenayya. 1996. "Improved ethanol tolerance and production in strains of *Clostridium thermocellum*." *World J Microbiol Biotechnol* no. 12:57-60.

Ratanakhanokchai, Khanok, Rattiya Waeonukul, Patthra Pason, Chakrit Tachaapaikoon, Khin Lay Kyu, Kazuo Sakka, Akihiko Kosugi, and Yutaka Mori. 2013.

"Paenibacillus curdlanolyticus Strain B-6 Multienzyme Complex: A Novel System for Biomass Utilization." In *Biomass Now - Cultivation and Utilization*, edited by Miodrag Darko Matovic.

Reviakine, I., D. Johannsmann, and R. P. Richter. 2011. "Hearing what you cannot see and visualizing what you hear: interpreting quartz crystal microbalance data from solvated interfaces." *Anal Chem* no. 83 (23):8838-48.

Rodahl, Michael, Fredrik Hook, Anatol Krozer, Peter Brzezinski, and Bengt Kasemoa. 1995. "Quartz crystal microbalance setup for frequency and Q factor measurements in gaseous and and liquid environments." *Rev. Sci. Instrum.* no. 66 (7):3924-3930.

Rojas, Orlando J., Changwoo Jeong, Xavier Turon, and Dimitris S. Argyropoulos. 2007. *Measurement of Cellulase Activity with Piezoelectric Resonators*. Vol. 954, *ACS Symposium*.

Rubin, E. M. 2008. "Genomics of cellulosic biofuels." *Nature* no. 454 (7206):841-5.

Ruel, K., Y. Nishiyama, and J. P. Joseleau. 2012. "Crystalline and amorphous cellulose in the secondary walls of Arabidopsis." *Plant Sci* no. 193-194:48-61.

Sauerbrey, G.Z. 1959. "Use of quartz vibrator for weighing thin films on a microbalance." *Z.Phs.* no. 155:206-222.

Schofield, A. L., T. R. Rudd, D. S. Martin, D. G. Fernig, and C. Edwards. 2007. "Real-time monitoring of the development and stability of biofilms of Streptococcus mutans using the quartz crystal microbalance with dissipation monitoring." *Biosens Bioelectron* no. 23 (3):407-13.

Shao, Xiongjun, Babu Raman, Mingjun Zhu, Jonathan Mielenz, Steven Brown, Adam Guss, and Lee Lynd. 2011. "Mutant selection and phenotypic and genetic characterization of ethanol-tolerant strains of *Clostridium thermocellum*." *Appl Microbiol Biotechnol* no. 92 (3):641-652.

Shin, D.G. , A.R. Yoo, S.W. Kim, and D.R. Yang. 2006. "Cybernetic modeling of simultaneous saccharification and fermentation for ethanol production from steam-exploded wood with *Brettanomyces custersii*." *J Microbiol Biotechn* no. 16:1355-1361.

Shoham, Yuval, Raphael Lamed, and Edward A. Bayer. 1999. "The cellulosome concept as an efficient microbial strategy for the degradation of insoluble polysaccharides." *Trends in microbiology* no. 7 (7):275-280.

Shuler, Michael L., and Fikret Kargi. 2002. *Bioprocess Engineering: Basic Concepts*: Prentice Hall.

Sun, Ye, and Jiayang Cheng. 2002. "Hydrolysis of lignocellulosic materials for ethanol production: a review." *Bioresource Technology* no. 83:1-11.

Taherzadeh, Mohammad J., and Keikhosro Karimi. 2007. "Enyme-based hydrolysis process for ethanol from lignocellulosic materials: a review." *BioResources* no. 2 (4):707-738.

Teugjas, H., and P. Valjamae. 2013. "Product inhibition of cellulases studied with 14C-labeled cellulose substrates." *Biotechnol Biofuels* no. 6 (1):104.

Tokatlidis, K., S. Salamitou, P. Beguin, P. Dhurjati, and J. P. Aubert. 1991. "Interaction of the duplicated segment carried by *Clostridium thermocellum* cellulases with cellulosome components." *FEBS Lett.* no. 29:185-188.

Tuka, K., V. V. Zverlov, and G. A. Velikodvorskaya. 1992. "Synergism between *Clostridium thermocellum* cellulases cloned in *Escherichia coli*." *Appl.Biochem. Biotechnol.* no. 37:201-207.

Turon, Xavier, Orlando J. Rojas, and Randall S. Deinhammer. 2008. "Enzymatic Kinetics of Cellulose Hydrolysis A QCM-D Study." *Langmuir* no. 24:3880-3887.

Valjamae, P., K. Kipper, G. Pettersson, and G. Johansson. 2003. "Synergistic cellulose

hydrolysis can be described in terms of fractal-like kinetics." *Biotechnol Bioeng* no. 84 (2):254-7.

Vasquez, Mariana Penuela, Juliana da Silva, MaurÃcio de Souza, and Nei Pereira. 2007. "Enzymatic hydrolysis optimization to ethanol production by simultaneous saccharification and fermentation." *Appl Biochem Biotech* no. 137 (1-12):141-153.

Voinova, M.V., M. Jonson, and B. Kasemo. 2002. "'Missing mass' effect in biosensor's QCM applications." *Biosensors and Bioelectronics* no. 17:835-841.

Wang, K., H. Y. Yang, F. Xu, and R. C. Sun. 2011. "Structural comparison and enhanced enzymatic hydrolysis of the cellulosic preparation from Populus tomentosa Carr., by different cellulose-soluble solvent systems." *Bioresour Technol* no. 102 (6):4524-9.

Wegener, Joachim, Andreas Janshoff, and Claudia Steinem. 2001. "The Quartz Crystal Microbalance as a Novel Means to Study Cell–Substrate Interactions In Situ." *Cell Biochemistry and Biophysics* no. 34:121-151.

Xi, Jun, Wenjian Du, and Linghao Zhong. 2013. "Probing the Interaction Between Cellulose and Cellulase with a Nanomechanical Sensor." In *Cellulose - Medical, Pharmaceutical and Electronic Applications*, edited by Dr. Theo G.M. Van De Ven. InTech.

Xu, C., Y. Qin, Y. Li, Y. Ji, J. Huang, H. Song, and J. Xu. 2010. "Factors influencing cellulosome activity in consolidated bioprocessing of cellulosic ethanol." *Bioresour Technol* no. 101 (24):9560-9.

Xu, Feng, and Hanshu Ding. 2007. "A new kinetic model for heterogeneous (or spatially confined) enzymatic catalysis: Contributions from the fractal and jamming (overcrowding) effects." *Applied Catalysis A: General* no. 317 (1):70-81.

Xu, Qi, A. Singh, and M. E. Himmel. 2009. "Perspectives and new directions for the production of bioethanol using consolidated bioprocessing of lignocellulose."

Curr Opin Biotechnol no. 20 (3):364-71.

Yaron, S., E. Morag, E. A. Bayer, R. Lamed, and Y. Shoham. 1995. "Expression, purification and subunit-binding properties of cohesins 2 and 3 of the *Clostridium thermocellum* cellulosome." *FEBS Lett.* no. 360:121–124.

Zhang, Wei, and Anli Geng. 2012. "Improved ethanol production by a xylosefermenting recombinant yeast strain constructed through a modified genome shuffling method." *Biotechnology for Biofuels* no. 5 (46).

Zhang, Y. H., and L. R. Lynd. 2005. "Cellulose utilization by Clostridium thermocellum: bioenergetics and hydrolysis product assimilation." *Proc Natl Acad Sci U S A* no. 102 (20):7321-5.

Zhong, Linghao, James F. Matthews, Michael F. Crowley, Tauna Rignall, César Talón, Joseph M. Cleary, Ross C. Walker, Giridhar Chukkapalli, Clare McCabe, Mark R. Nimlos, Charles L. Brooks, Michael E. Himmel, and John W. Brady. 2007. "Interactions of the complete cellobiohydrolase I from Trichodera reesei with microcrystalline cellulose Iβ." *Cellulose* no. 15 (2):261-273.

Zhou, J, YH Wang, J Chu, LZ Luo, YP Zhuang, and SL Zhang. 2009. "Optimization of cellulase mixture for efficient hydrolysis of steam-exploded corn stover by statistically designed experiments." *Bioresource Technol* no. 100:819-825.

<div align="center">

VITA

Shanshan Zhou

</div>

Place of Birth: Fujiang, China

Educational institutions attended and degrees already awarded:

Bachelor of Science in Chemical Engineering, East China University of Science and Technology, Shanghai, China (2012)

Professional Positions:

Graduate Research Assistant, Chemical and Material Engineering Department, University of Kentucky (December, 2012-Present).

Teaching Assistant, Chemical and Material Engineering Department, University of Kentucky (August, 2012-May, 2013).

Undergraduate Research Assistant, Chemical Engineering Department, East China University of Science and Technology (December, 2011-June, 2012).

Scholastic and Professional Honors:

Outstanding Student Award in Science and Engineering of ECUST (2012)

First-class Scholarship, East China University of Science and Technology (2008-2012).

Professional Publications and Presentations:

S. Zhou, R. Garlapalli, S. E. Rankin and B. L. Knutson. "Quartz Crystal Microbalance Investigation of *C.thermocellum* Activity and Inhibition by Cellobiose on Model Cellulose Surface", Chemical & Materials Engineering Department Poster Session, Lexington, KY, Sep, 2013.

<div align="right">

Shanshan Zhou

July 7, 2014

</div>